



Nonsmooth one-dimensional maps: some basic concepts and definitions

I. Sushko, L. Gardini & V. Avrutin

To cite this article: I. Sushko, L. Gardini & V. Avrutin (2016): Nonsmooth one-dimensional maps: some basic concepts and definitions, *Journal of Difference Equations and Applications*, DOI: [10.1080/10236198.2016.1248426](https://doi.org/10.1080/10236198.2016.1248426)

To link to this article: <http://dx.doi.org/10.1080/10236198.2016.1248426>



Published online: 24 Oct 2016.



Submit your article to this journal 



Article views: 22



View related articles 



View Crossmark data 

Nonsmooth one-dimensional maps: some basic concepts and definitions

I. Sushko^a, L. Gardini^b and V. Avrutin^c

^aInstitute of Mathematics, National Academy of Sciences of Ukraine, Kyiv, Ukraine; ^bDESP, University of Urbino, Urbino, Italy; ^cIST, University of Stuttgart, Stuttgart, Germany

ABSTRACT

The main purpose of the present survey is to contribute to the theory of dynamical systems defined by one-dimensional *piecewise monotone maps*. We recall some definitions known from the theory of *smooth* maps, which are applicable to piecewise smooth ones, and discuss the notions specific for the considered class of maps. To keep the presentation clear for the researchers working in other fields, especially in applications, many examples are provided. We focus mainly on the notions and concepts which are used for the investigation of various kinds of attractors of a map and related bifurcation structures observed in its parameter space.

ARTICLE HISTORY

Received 6 October 2016
Accepted 7 October 2016

KEYWORDS

Piecewise smooth map;
border collision bifurcation;
homoclinic bifurcation;
bifurcation structure

AMS SUBJECT CLASSIFICATIONS

37E05; 37G35; 37N30

1. Introduction

Dynamical systems defined by *nonsmooth functions*, *continuous or discontinuous*, are nowadays actively studied by many scientists from various theoretical and applied research fields. In fact, many real processes characterized by nonsmooth phenomena, such as sharp switching, impacts, friction, sliding, etc., are successfully modelled by piecewise smooth functions. Among numerous examples we can mention switching electronic circuits, such as DC–DC converters, mechanical systems with impacts or stick–slip motion, relay control systems, etc. (for the related references and further examples from electronics, mechanics, control and other fields see [15,22,80]). In economics, piecewise smooth dynamical systems appear naturally as different constraints become binding in different regimes. For example, in models of innovation dynamics in [35,47,56,60], kinks appear as the economy hits the non-negativity constraint on innovation. In models of investment dynamics under financial frictions in [1,57–59,61], kinks or discontinuities appear as various financing constraints become binding. For other applications in economics, see [18].

The theory of nonsmooth dynamical systems is still far from being complete. Regarding piecewise smooth *continuous-time* systems (flows) it is worth to mention [15], where *discontinuity-induced bifurcations* are introduced and classified, being associated with discontinuous derivative of the function defining a nonsmooth system. In earlier works, such as [50] (see also [36]), various bifurcation structures in nonsmooth continuous and discontinuous one-dimensional (1D) maps are described, and in [30] (see also [16])

bifurcations occurring in nonsmooth n -dimensional continuous systems (called there C-bifurcations) are classified. We mention also [12,22,80], which discuss different aspects of theory and applications of piecewise smooth systems.

The term *border collision bifurcation* (BCB) (see [67,68]) is used for *discrete-time* dynamical systems to indicate bifurcations occurring when an invariant set collides with a border at which the system changes the function in its definition, and this collision leads to a qualitative change in the topological structure of the state space. The theory of BCBs is well developed for 1D continuous maps (see, e.g. [75] and references therein) while for higher-dimensional and especially for discontinuous maps, there are still many open problems.

In the present survey we consider discrete-time dynamical systems defined by 1D *piecewise monotone maps*. Our main purpose is to recall some well-known definitions from the theory of *smooth* maps, which are applicable to piecewise smooth maps without significant changes, and discuss the notions which either require certain extensions for the considered class of maps (as, e.g. the notion of critical point), or just do not exist in the theory of smooth maps (as, e.g. the notion of BCB or Cantor set attractor). To keep the presentation clear for the researchers working in other fields, especially in applications, we provide many examples, with focus on the notions and concepts which are used for the investigation of various kinds of attractors of a map and related bifurcation structures observed in its parameter space. By *bifurcation structure* we mean a partitioning of the parameter space into regions associated with qualitatively similar asymptotic dynamics.

As an example of a 1D smooth map, we use the well-known *logistic map* $q : [0, 1] \rightarrow [0, 1]$, defined as

$$x_{n+1} = q(x_n), \quad q(x) = \alpha x(1 - x), \quad (1)$$

where α is a real parameter, $0 < \alpha < 4$ (some comments on the case $\alpha \geq 4$ are also given). As an example of 1D nonsmooth map, we consider a 1D *piecewise linear* map $f : I \rightarrow I$, $I \subseteq \mathbb{R}$, defined on two partitions:

$$x_{n+1} = f(x_n) = \begin{cases} f_L(x_n) = a_L x_n + \mu_L & \text{if } x_n < 0 \\ f_R(x_n) = a_R x_n + \mu_R & \text{if } x_n > 0 \end{cases} \quad (2)$$

where a_L, a_R, μ_L, μ_R are real parameters. The map (2) belongs to the class of 1D *piecewise smooth* maps $g : I \rightarrow I$, $I \subseteq \mathbb{R}$, defined by two monotone functions g_L and g_R in two sub-intervals I_1 and I_2 , respectively, $I_1 \cup I_2 = I$, separated by a *border point* which, without loss of generality, can be translated to the origin:

$$x_{n+1} = g(x_n) = \begin{cases} g_L(x_n) & \text{if } x_n < 0 \\ g_R(x_n) & \text{if } x_n > 0 \end{cases} \quad (3)$$

The value of the functions f and g at $x = 0$ are intentionally not specified, as both limit values at the border point are valid for the description of various bifurcations, and orbits of both limit values are often important for the description of the dynamics of the map.

Map (2) in the *continuous* case ($\mu_L = \mu_R =: \mu$) represents the well-known *skew tent map*

$$x_{n+1} = f(x_n) = \begin{cases} f_L(x_n) = a_L x_n + \mu & \text{if } x_n \leq 0 \\ f_R(x_n) = a_R x_n + \mu & \text{if } x_n \geq 0 \end{cases} \quad (4)$$



The bifurcation structure of the parameter space of this map is completely described (see, e.g. [45,53,68]), and this fact helps to use of the skew tent map as a *border collision normal form* by means of which a generic BCB in map (3) in the continuous case $g_L(0) = g_R(0)$ can be classified (see [75] for a survey).

To give a complete description of the overall bifurcation structure for maps f and g in the *discontinuous* case is a challenging task. It is already done for some cases, in particular, for the maps with increasing/increasing and increasing/decreasing *contracting* branches, characterized by periodicity regions, related to attracting cycles, which are organized in so-called *period adding* and *period incrementing* structures, respectively (see, e.g. [33] and references therein, where these structures are associated with codimension-two BCB points). For piecewise linear maps (particular cases of map (2)) so-called *bandcount adding* and *bandcount incrementing* structures formed by chaotic attractors are described in [9,10] and [4–6], respectively. However, there are still several open problems concerning mixed type bifurcation structures, especially those associated with generic piecewise smooth maps.

The paper is organized as follows. After some preliminaries presented in Section 2, where we recall, among others, such notions as critical point and absorbing interval, we discuss in Section 3 possible kinds of attractors which a piecewise smooth 1D map, continuous or discontinuous, can possess. Then, in Section 4 different kinds of basins of attraction of such attractors are presented. Section 5 deals with repellors and other invariant sets. In Section 6 we recall the notion of a homoclinic orbit and homoclinic bifurcation, which are important not only as an instrument to prove that a map is chaotic, but also for the detection of the conditions of various bifurcations of chaotic attractors, namely, *merging*, *expansion* and *final* bifurcations. We discuss such bifurcations as well as other properties of chaotic attractors in Section 7. Coexistence of several attractors in a 1D map is addressed in Section 8. In Section 9 we recall the notion of the first return map which often helps to simplify investigation of the dynamics of a map. Section 10 can be seen as an example how the notions and concepts discussed in the present paper can be used for the study of the dynamics of a particular class of 1D maps, namely, piecewise increasing maps. Section 11 concludes.

2. Preliminaries

2.1. Orbits and their limit sets

Let us first recall the simplest notions relevant for the description of the dynamics of a generic 1D map $f : I \rightarrow I$, $I \subset \mathbb{R}$ (see, e.g. [28,41,65,71]).

A point $x_0 \in I$ is transformed in one iteration by map f into a point $x_1 = f(x_0) \in I$ called *rank-one (forward) image* of x_0 . Any point x_0 such that $f(x_0) = x_1$ is a *rank-one preimage* of x_1 . The (forward) iterations by f of an initial point $x_0 \in I$ define uniquely an *orbit* $\mathcal{O}(x_0) = \{x_i\}_{i=0}^{\infty}$, where $x_i = f^i(x_0)$, f^0 is the identity function and $f^i = f \circ f^{i-1}$ is the i th iterated of f .

The simplest orbits are a *fixed point* $x = x^*$ (satisfying $f(x) = x$), and a periodic orbit, or *cycle*, of period n (n -cycle for short), $n > 1$, which is a set $\mathcal{O} = \{x_i\}_{i=0}^{n-1}$ of n distinct points satisfying $f(x_i) = x_{i+1}$, $i = 0, \dots, n-2$, $f(x_{n-1}) = x_0$. Given that $f^n(x_i) = x_i$, an n -cycle corresponds to n related fixed points of the n th iterate f^n .

A set $E \subset I$ is *invariant* by the map f if $f(E) = E$. This means that if $x \in E$ then $f(x) \in E$, and each point of E is the forward image of at least one point of E . The simplest examples of invariant sets of a map are its fixed points and cycles.

As we are interested in the *asymptotic behaviour* of the orbits, recall that the ω -*limit set* of an orbit $\mathcal{O}(x_0)$, denoted $\omega(x_0)$, is the set of all accumulation points of this orbit under forward iterations. More formally, a point $q \in \omega(x_0)$ if there exists an increasing sequence $i_1 < i_2 < \dots < i_k < \dots$ such that $f^{i_k}(x_0) \rightarrow q$ as $k \rightarrow \infty$. The set $\omega(x_0)$ is invariant and can be considered as representative of the long-term behaviour of $\mathcal{O}(x_0)$. The α -*limit set* of an orbit $\mathcal{O}(x_0)$, denoted $\alpha(x_0)$, consists of the accumulation points of the set of preimages $\cup_{i \geq 0} f^{-i}(x_0)$. Here the inverse function f^{-i} is uniquely defined iff f is invertible. Otherwise, the function f^{-i} is multivalued, so that $f^{-i}(x_0)$ may be a set of points.

It is known that the dynamics of a map strongly depend on whether the map is invertible or noninvertible, continuous or discontinuous. For continuous invertible 1D maps defined in $I \subset \mathbb{R}$ the asymptotic behaviour of orbits is rather trivial: the ω -limit set of any bounded orbit is either a fixed point or a period-2 cycle. The dynamics of a discontinuous map which is invertible in I may be more complicated: the ω -limit set of an orbit may be a cycle of any period, or a *Cantor set attractor* (its definition is recalled in Section 3.3). However, neither continuous nor discontinuous 1D maps invertible in I can be chaotic. That means, noninvertibility of a 1D map is an essential property for chaotic dynamics.

Recall also an important notion of topological conjugacy which helps to identify maps with qualitatively similar dynamics. A map $f : X \rightarrow X$ is *topologically conjugate* to a map $g : Y \rightarrow Y$, where X, Y are topological spaces, if there exists a homeomorphism (a function which is continuous and has a continuous inverse) $h : Y \rightarrow X$ such that $f \circ h = h \circ g$. Topologically conjugate maps have qualitatively the same dynamics, since their orbits are in one-to-one correspondence via h .

2.2. Critical points

In the study of 1D maps (smooth or piecewise smooth, continuous or discontinuous) a significant role is played by so-called *critical points*, as well as their forward and backward images. Using such points one can determine the boundaries of absorbing intervals and chaotic attractors; they are used also to obtain conditions of homoclinic bifurcations, BCBs, etc.

There are several concepts of a critical point. According to the most spread definition, a *critical point* of a continuous function $f(x)$ is an inner point of the definition region I of $f(x)$ at which the first derivative of $f(x)$ is either zero or not defined. Such a definition includes points of local extrema, inflection points and points of nondifferentiability of the function. In the context of dynamical systems theory, mainly points of local extrema (sometimes called also as *fold points*) are taken into account. To give an example, for the logistic map (1) the critical point according to the above definition is $x = \frac{1}{2}$.

A different definition of a critical point goes back to the French school of iteration theory. According to the definition used by Julia, Fatou and other authors in their studies of complex maps (see [29,48]),

Definition 1: A **critical point** of zero-rank of a continuous function $f(x)$ is a point $x = c$ which has at least two merging rank-one preimages.

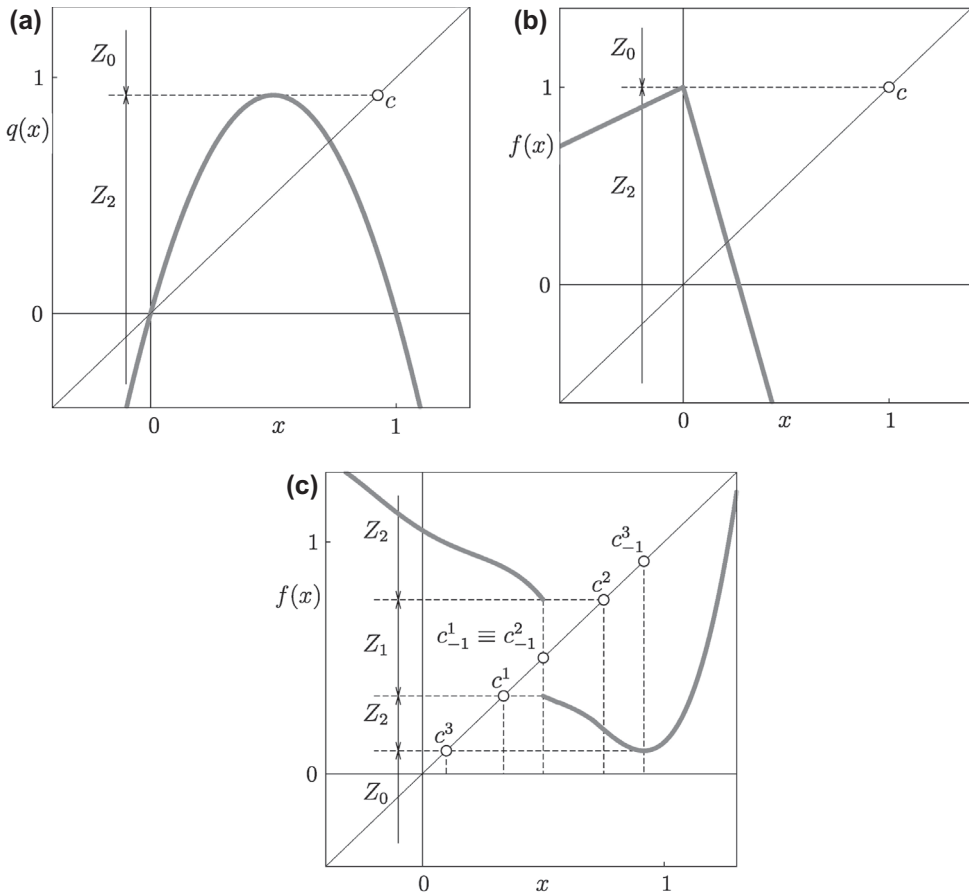


Figure 1. The logistic map (a) and the skew tent map (b) belong to the class of noninvertible maps of the Z_0-Z_2 type; in both cases, the critical point c is the maximum of the function. In (c): A discontinuous map of the type $Z_0-Z_2-Z_1-Z_2$ is shown, with critical points c^1 , c^2 (limit values of the function at the discontinuity point) and c^3 ('smooth' local minimum).

In this way a critical point is defined as the *value* of the function at a point of a local extremum, moreover, the inflection points as well as the kink points which are not related to an extremum, are excluded from the consideration (see also [65,66]).

The reason why this definition does not consider the *point* of local extremum to be critical but the *value* of the function at this point, is illustrated in Figure 1: critical points divide the definition region I of the function in sub-intervals whose points have different numbers of preimages. From a geometrical point of view, as a result of the action of a noninvertible continuous map, interval I is folded at the critical points. For example, for the logistic map (1) its unique critical point $c = \frac{\alpha}{4}$ separates two intervals: any point $x \in Z_0 = (c, \infty)$ has no preimage, while any $x \in Z_2 = (-\infty, c)$ has two different preimages (see Figure 1(a)). Therefore, the logistic map belongs to the class of noninvertible maps of the so-called Z_0-Z_2 type (see [66]). Similar conclusions hold for the skew tent map (4) when the slopes of the functions f_L and f_R have different signs, that is, if $\alpha_L \alpha_R < 0$. In such a case the point $f_L(0) = f_R(0) = \mu$ is a critical point, $c = \mu$, and f is a noninvertible map of Z_0-Z_2 type (see Figure 1(b)).

Note that at the point of a local extremum a function may be neither smooth (as for the skew tent map mentioned above), nor continuous: indeed, a function f is said to have a local maximum (resp., minimum) at the point $x = \hat{x}$ if there exists $\epsilon > 0$ such that $f(\hat{x}) \geq f(x)$ (resp., $f(\hat{x}) \leq f(x)$) when $|x - \hat{x}| < \epsilon$. However, if $x = \hat{x}$ is a point of discontinuity, it may be associated with two extrema: it may happen that there exists $\epsilon > 0$ such that for $|x - \hat{x}| < \epsilon$ it holds that $f(\hat{x}_-) \geq f(x)$ while $f(\hat{x}_+) \leq f(x)$. For example, if both functions $f_L(x)$ and $f_R(x)$ of map (2) are increasing and $f_L(0) > f_R(0)$, then for a neighbourhood of the discontinuity point $x = 0$ it holds that $f(0_-) \geq f(x)$ while $f(0_+) \leq f(x)$, or if both functions $f_L(x)$ and $f_R(x)$ are decreasing and $f_L(0) < f_R(0)$, the inequalities $f(0_+) \geq f(x)$ and $f(0_-) \leq f(x)$ are satisfied. Moreover, both values $f(0_-) = f_L(0)$ and $f(0_+) = f_R(0)$ separate intervals with different number of preimages, so that map (2) has $Z_1 - Z_2 - Z_1$ type of noninvertibility (see e.g. Figure 3).

It is clear that for a generic discontinuous map f with a discontinuity point $x = \hat{x}$, each of the limit values of f at $x = \hat{x}$, say, $c^\ell := f(\hat{x}_-)$ or $c^r := f(\hat{x}_+)$, separates two intervals, I_1 and I_2 , associated with different inverses of f , moreover, in the generic case the number of such inverses, or, in other words, the number of preimages for points in I_1 and I_2 , is different (it may also happen that points of one of the intervals have no preimages). This fact may be quite important for the description of the dynamics of the map, therefore, both limit values of the function at the discontinuity point have to be taken into consideration. As an example, in Figure 1(c) we show a discontinuous map with three critical points: c^1 and c^2 are limit values of the function at the discontinuity point, and c^3 is a ‘smooth’ local minimum.¹

So, in the present paper we use the following definition of a critical point:

Definition 2: For a 1D continuous map its local extrema are called **critical points**. For a 1D discontinuous map, besides the critical points associated with its continuous branches, the limit values of the function at the discontinuity points are also called **critical points**.

Note that critical points may be associated also with a vanishing denominator of the map or one of its inverses (see [19,34]), however, such cases are not considered in the present paper.

The rank- i image of a critical point c is denoted as c_i , that is, $c_i = f^i(c)$, $i \geq 1$. A rank- i preimage of a critical point c is a point x which satisfies $f^i(x) = c$. In general a critical point may have zero, one or several preimages of rank i , $i > 1$. In the following a preimage of a critical point of rank i , $i \geq 1$, is denoted by c_{-i} , and if there are several preimages of the same rank i , we distinguish between them using additional indexes. A point of ‘continuous’ local extremum, as well as a point of discontinuity, is denoted as c_{-1} .

2.3. Absorbing intervals

To study the dynamics of a 1D map $f : I \rightarrow I$, $I \subset \mathbb{R}$, it is worth to identify first the intervals to which the asymptotic behaviour is confined, and to which the analysis can be restricted. In this context, the concept of an absorbing interval is useful.

Definition 3: An interval J is said to be **absorbing** if

- (a) $f(J) \subseteq J$ (i.e. either J is invariant, $f(J) = J$, or it is strictly mapped into itself, $f(J) \subsetneq J$);

- (b) a neighbourhood \mathcal{U} of J exists such that for any $x \in \mathcal{U}$ there exists a *finite* integer $k > 0$ such that $f^k(x) \in J$ (i.e. any point $x \in \mathcal{U}$ is mapped inside J in a finite number of iterations);
- (c) J is bounded by two different critical points, or a critical point and its image.

For example, the absorbing interval J of the skew tent map (4) in the case $a_L > 0, a_R < 0, \mu > 0$ is bounded by the critical point $c = \mu$ and its rank-one image $c_1 = f(c) = \mu(a_R + 1)$, $J = [c_1, c]$. It is known (see, e.g. [75]) that

- if $-1 < a_R < 0, 0 < a_L < 1$ the interval J is *absorbing but not invariant*, that is, $f(J) \subsetneq J$, and the unique attractor of f is the attracting fixed point $\mathcal{O}_R = \mu/(1 - a_R)$ to which the interval J shrinks under the iterations (see Figure 2(a)).
- if $a_R < -1, 0 < a_L < 1$ then J is a *globally attracting invariant absorbing interval* (see Figure 2(b)). It is mapped onto itself, $f(J) = J$, and any initial point $x_0 \notin J$ is mapped inside J in a finite number of iterations. The attractor of f , belonging to J , is either an attracting cycle, or a chaotic attractor.
- for $a_R < -1, a_L > 1$ the map f has one more fixed point $\mathcal{O}_L = \mu/(1 - a_L)$, which is repelling. As long as $c_1 > \mathcal{O}_L$ (this case is not shown in Figure 2), the interval J remains *an invariant absorbing interval* but it is *no longer globally attracting*. Its basin of attraction is bounded by point \mathcal{O}_L and its rank-one preimage. As both slopes of f are larger than 1 in modulus, the map f cannot have an attracting cycle, but only a chaotic attractor (chaotic intervals).
- for $a_R < -1, a_L > 1$ and $c_1 < \mathcal{O}_L$ the interval J is *no longer an absorbing interval*, $f(J) \supsetneq J$ (see Figure 2(c)). The generic initial point $x_0 \in J$ is mapped outside J in a finite number of iterations and leads to a divergent orbit. However, not all the orbits with an initial point in J are divergent: J contains an invariant Cantor set which is a so-called chaotic repeller.

Two more examples are shown in Figure 3: for $0 < a_L < 1, 0 < a_R < 1, \mu_L > 0$ and $\mu_R < 0$ map (2) has no fixed points, and the invariant absorbing interval $J = [\mu_R, \mu_L]$ is globally attracting (see Figure 3(a)); for $a_L > 1, a_R > 1, \mu_L > 0$ and $\mu_R < 0$ map (2) has two repelling fixed points, \mathcal{O}_L and \mathcal{O}_R , which are boundaries of the basin of attraction of the invariant absorbing interval $J = [\mu_R, \mu_L]$ as long as the inequalities $\mu_L < \mathcal{O}_R$ and $\mu_R > \mathcal{O}_L$ hold (see Figure 3(b)). As recalled in Section 10, in the first case an attractor of map (2) is either an attracting cycle, or a Cantor set attractor, while in the second case the only possible attractor of the map is a chaotic attractor.

3. Attracting sets and attractors

There are several different concepts of an attractor. In the present paper we use the following one:

Definition 4: (a) An **attracting set** A of a map $f : I \rightarrow I, I \subseteq \mathbb{R}$, is a closed invariant set for which a neighbourhood $\mathcal{U}(A)$ exists such that $f(\mathcal{U}(A)) \subset \mathcal{U}(A)$ and $f^n(x) \rightarrow A$ as $n \rightarrow \infty$ for any $x \in \mathcal{U}(A)$; (b) An **attractor** \mathcal{A} is an attracting set with a dense orbit.

It is important to note that an attracting set may contain one or several attractors, repelling cycles or more complicated invariant subsets, whereas an attractor is an undecomposable set.

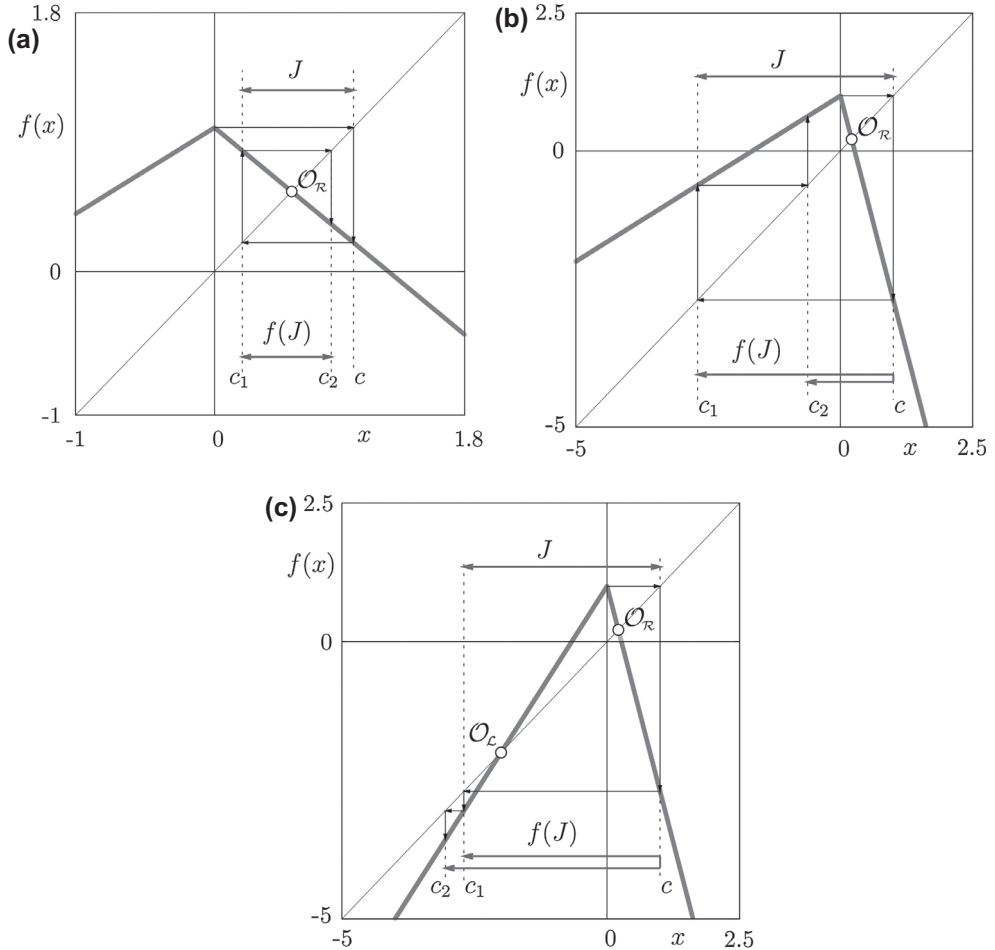


Figure 2. The interval $J = [f(c), c]$, $c = \mu$, for map (4) is (a) an absorbing but not invariant interval, $f(J) \subset J$; (b) an absorbing invariant interval, $f(J) = J$; (c) neither invariant, nor absorbing, $f(J) \supset J$. Parameters: $\mu = 1$ and $a_L = 0.6$, $a_R = -0.8$ in (a), $a_L = 0.6$, $a_R = -0.43$ in (b), and $a_L = 1.5$, $a_R = -3.7$ in (c).

Without going into a detailed discussion on other definitions of an attractor, we mention only the one proposed by Milnor (see [64]) and called after him a *Milnor attractor*, or also a *measure attractor*.

Definition 5: A **Milnor attractor** is a closed invariant set $\mathcal{A} \subset I$ such that its stable set $W^s(\mathcal{A})$ (consisting of all points $x \in I$ for which $\omega(x) \subset \mathcal{A}$) has a strictly positive measure, and there is no strictly smaller closed subset \mathcal{A}' of \mathcal{A} such that $W^s(\mathcal{A}')$ coincides with $W^s(\mathcal{A})$ except for a set of measure zero.

Obviously, any set \mathcal{A} which is an attractor according to Definition 4 is also a Milnor attractor, but not vice versa. If \mathcal{A} is a Milnor attractor but not an attractor in the sense of Definition 4, then some (or even all) orbits $\mathcal{O}(x)$ for $x \in \mathcal{U}(\mathcal{A}) \setminus \mathcal{A}$ leave $\mathcal{U}(\mathcal{A})$ within a finite number of iterations (although they may be eventually mapped into \mathcal{A}).

According to Definition 4, for 1D continuous maps there are attractors of two types,² namely attracting n -cycles and n -band chaotic attractors (or n cyclic chaotic intervals),

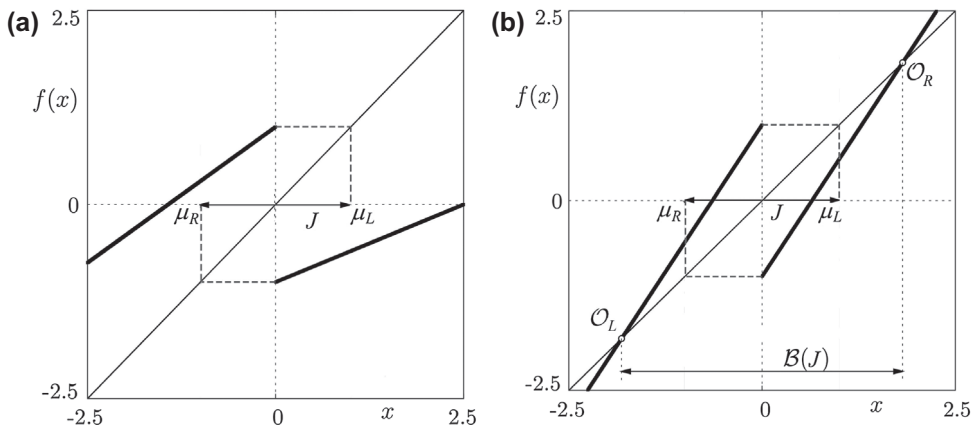


Figure 3. Absorbing interval $J = [\mu_R, \mu_L]$ of map (2). In (a) the interval J is globally attracting. In (b) repelling fixed points O_L and O_R confine the basin of attraction $B(J)$ of J (set of points with $\omega(x) \subset J$). Parameters: $\mu_L = 1$, $\mu_R = -1$ and $a_L = 0.7$, $a_R = 0.4$ in (a), $a_L = a_R = 1.55$ in (b).

$n \geq 1$. *Discontinuous maps*, besides attracting cycles and n -band chaotic attractors (which may be cyclic or not, as we discuss in Section 7.3), can have two more types of attractors, both associated with quasiperiodic orbits, namely Cantor set attractors and attracting intervals densely filled with quasiperiodic orbits. Below we discuss these four types of attractors in turn.

3.1. Attracting cycles

Let $\mathcal{O} = \{x_i\}_{i=0}^{n-1}$ be an n -cycle of a 1D map f . If no one periodic point coincides with a point of non-differentiability of the map, that is, with a kink or discontinuity point, then the *eigenvalue* (or *multiplier*) of this cycle is well defined and given by $\lambda(\mathcal{O}) = (f^n)'(x_i)$ for any $i = 0, \dots, n-1$, or, $\lambda(\mathcal{O}) = \prod_{i=0}^{n-1} f'(x_i)$. In such a case, if $|\lambda(\mathcal{O})| \neq 1$ the cycle \mathcal{O} is called *hyperbolic*, otherwise it is a *nonhyperbolic* (or *neutral*) cycle, and a sufficient condition for \mathcal{O} to be asymptotically stable, i.e. attracting, is $|\lambda(\mathcal{O})| < 1$. This is not a necessary condition, as for example, a nonhyperbolic cycle undergoing a supercritical flip bifurcation or a supercritical pitchfork bifurcation is asymptotically stable.

If one of the points of a cycle \mathcal{O} coincides with a kink point $x = \hat{x}$ of map f , say, $x_0 = \hat{x}$, one still can discuss local attractivity of such a cycle considering the one-side derivatives $(f^n)'(\hat{x}_-)$ and $(f^n)'(\hat{x}_+)$: if both these values are less than 1 in modulus, then \mathcal{O} is attracting. If $x = \hat{x}$ is a discontinuity point and $x_0 = \hat{x}$, only one one-side derivative can be evaluated. Indeed, if under variation of a parameter some point of \mathcal{O} collides with a border point (i.e. a kink or discontinuity point), and such a collision leads to a qualitative change of the dynamics, then we say that the cycle \mathcal{O} undergoes a BCB.

3.2. Chaotic attractors

One of the most widespread definition of chaos is given by Devaney (see e.g. [28]):

Definition 6: A continuous map $f : X \rightarrow X$, $X \subseteq \mathbb{R}$, is **chaotic** on a closed invariant set X if

- (1) f is topologically transitive;
- (2) periodic points of f are dense in X ;
- (3) f has sensitive dependence on initial conditions.

A chaotic attractor is an attracting set X on which f is chaotic.

In [14] it is shown that in nondegenerate cases the properties (1) and (2) imply the property (3), which is therefore redundant. In [2] it is shown that for a generic map this is the only redundancy in Devaney's definition. However, for *continuous maps on an interval*, $I = X$, it is proved in [78] that property (1) implies properties (2) and (3), so that for such maps the topological transitivity can be seen as a definition of chaos. Recall that *topological transitivity* in I means that for any two non-empty open sets $U, V \subset I$ an integer m exists such that $f^m(U) \cap V \neq \emptyset$, and in fact it is equivalent to the existence of an aperiodic orbit (that means neither periodic, nor quasiperiodic) which is dense on I . For *discontinuous maps on an interval* the properties (1) and (2) are both necessary for a definition of chaos.

It is worth mentioning that Devaney's definition of chaos is not the unique one in the literature. Depending on the particular research field and problem, other definitions are used as well, such as, for example, the one given by Li and Yorke [51]. Quite widespread are also the definitions based on the equivalence of the map to a shift on a sequence space [20], and on an absolutely continuous invariant measure [46]. There is also a definition of chaos based on rotation numbers [49], convenient for investigation of maps for which the concept of a rotation number can be naturally introduced, as, for example, for map (2). In any case, independently of the used definition, there are two basic ingredients of chaos which are conventionally referred to as 'elements of regularity within chaos' and 'mixing property, or indecomposability'. With regard to a chaotic attractor \mathcal{A} , these ingredients are present in the form of a countable infinity of repelling cycles which are dense in \mathcal{A} (sometimes also referred to as the skeleton of the attractor), and an aperiodic orbit which is dense in \mathcal{A} .

Considering the geometric shape of a chaotic attractor, note that in 1D maps it is either an interval (bounded or unbounded), also called a *one-band attractor*, or a set of m intervals. As an example, Figure 4(a) shows a one-band chaotic attractor of the map (2) filling the complete invariant absorbing interval $I = [c_1, c]$ with $c = f_R(0)$, $c_1 = f_R^2(0)$. By contrast, the 20-band attractor shown in Figure 4(b) does not fill I completely and the bands are separated by 19 gaps.

A simple but important question arises whether the bands are mapped onto each other cyclically or not. In Section 7.3 (see also [11]) we show that in the continuous case the intervals of a multi-band chaotic attractor are always cyclic, while in the discontinuous case cyclicity may be lost.

3.3. Attractors related to quasiperiodic orbits

3.3.1. Cantor set attractors

Discontinuous 1D maps, additionally to attracting cycles and chaotic attractors, may have also Cantor set attractors defined as follows (see also [49]):

Definition 7: A **Cantor set attractor** is an attracting set homeomorphic to a Cantor set. It is the closure of quasiperiodic orbits.

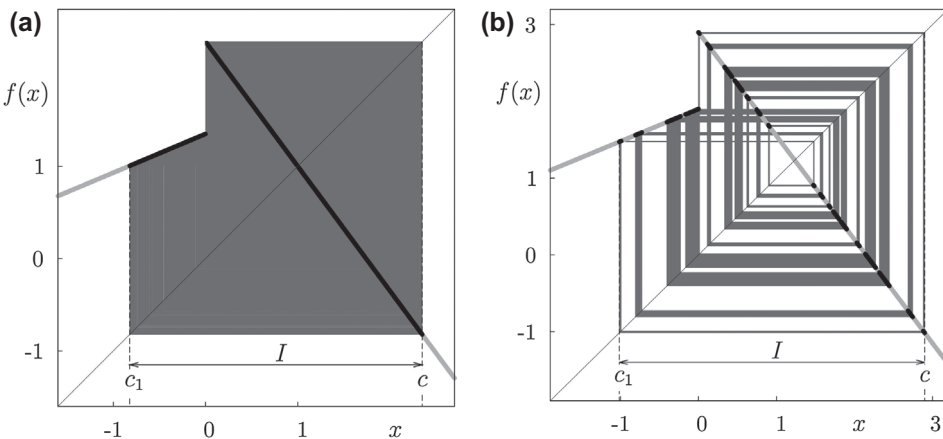


Figure 4. A one-band chaotic attractor (a), and a 20-band chaotic attractor (b) of map (2). Parameters: $a_L = 0.42$, $a_R = -1.35$, and $\mu_L = 1.35$, $\mu_R = 2.35$ in (a); $\mu_L = 1.9$, $\mu_R = 2.9$ in (b).

Note that Cantor set attractors in general do not persist under parameter perturbations. In Section 10 we discuss Cantor set attractors observed for a particular family of 1D piecewise increasing maps known as Lorenz maps.

3.3.2. Attracting intervals with quasiperiodic orbits

There is one more type of attractors in discontinuous maps which is also associated with quasiperiodic orbits, but, differently from the Cantor set attractor, it is an *attracting interval* representing the *closure of quasiperiodic orbits*. Consider, for example, a discontinuous map g given in (3), defined by two increasing functions $g_L(x)$ and $g_R(x)$ of class C^2 , such that at the discontinuity point $x = 0$ it holds $g_L(0) > 0$ and $g_R(0) < 0$. Let g in the absorbing interval $I = [g_R(0), g_L(0)]$ be *invertible* and *onto*, that is, $g_L(g_R(0)) = g_R(g_L(0))$ (and, thus, I is invariant). Then the map g , restricted to the invariant absorbing interval I , is conjugate to a circle homeomorphism $\tilde{g} : S^1 \rightarrow S^1$. As recalled in Section 10.3, if \tilde{g} has an *irrational* rotation number then any orbit of \tilde{g} is quasiperiodic and dense in I . There are infinitely many quasiperiodic orbits (each of them is dense in I), so that the ω -limit set of each orbit is the whole interval I . Thus, in the case of an irrational rotation the interval I is an attractor of the map (3). For the piecewise linear map (2) such a kind of attractors exists for parameter values associated with irrational rotation numbers, which belong to the set S related to the transition from invertibility to noninvertibility of f on the absorbing interval (and also from regular to chaotic dynamics). The set S is defined by the condition $f_L(f_R(0)) = f_R(f_L(0))$, or $\mu_R(1 - a_L) = \mu_L(1 - a_R)$. In general, such attractors do not persist under parameter perturbations.

4. Basins of attraction

Let \mathcal{A} be an attractor of a map $f : I \rightarrow I$, $I \subseteq \mathbb{R}$. It follows from Definition 4 that \mathcal{A} has a neighbourhood each point of which converges to the attractor. In fact,

Definition 8: The largest neighbourhood of \mathcal{A} each point of which converges to \mathcal{A} is called **immediate basin** $\mathcal{B}_0(\mathcal{A})$ of \mathcal{A} .

The *total basin of attraction* $\mathcal{B}(\mathcal{A})$ of \mathcal{A} , or simply the basin of attraction of \mathcal{A} is defined as follows:

Definition 9: The **basin of attraction** $\mathcal{B}(\mathcal{A})$ of \mathcal{A} is the set of all points converging to \mathcal{A} , i.e. the points whose ω -limit set belongs to \mathcal{A} .

Note that the basin of an attracting cycle \mathcal{A} consists of all the points whose ω -limit set *coincides* with \mathcal{A} . By contrast, for a *chaotic* attractor \mathcal{A} the basin also contains points whose ω -limit sets are strictly included in \mathcal{A} (such as, for example, preimages of repelling cycles belonging to \mathcal{A}).

The total basin $\mathcal{B}(\mathcal{A})$ of \mathcal{A} can be constructed in two steps:

- (1) detect the immediate basin $\mathcal{B}_0(\mathcal{A}) \subset \mathcal{B}(\mathcal{A})$;
- (2) take all the preimages of the immediate basin, so that the total basin is given by

$$\mathcal{B}(\mathcal{A}) = \bigcup_{i=0}^{\infty} f^{-i}(\mathcal{B}_0(\mathcal{A})), \quad (5)$$

where $f^{-i}(\mathcal{B}_0(\mathcal{A}))$ for $i = 0$ is the identity, and for $i \geq 1$ it represents the rank- i preimage(s) of the immediate basin (recall that for a noninvertible map a set may have several preimages of the same rank).

The immediate basin $\mathcal{B}_0(\mathcal{A})$ of a *simply-connected attractor* \mathcal{A} is an open interval which can be either bounded, or unbounded. For a *continuous* map the bounded interval $\mathcal{B}_0(\mathcal{A})$ can be confined by

- (a) two repelling (at least, from one side) fixed points (Figure 5(a));
- (b) a repelling (at least, from one side) fixed point and its rank-1 preimage (Figure 5(b));
- (c) two points of a repelling 2-cycle (Figure 5(c)).

In the unbounded case $\mathcal{B}_0(\mathcal{A})$ can be either two-side unbounded, or bounded on one side by a repelling fixed point and unbounded on the other side.

The immediate basin $\mathcal{B}_0(\mathcal{A})$ of a simply-connected attractor \mathcal{A} of a *discontinuous* map, besides the cases listed above can also be bounded by

- (d) a discontinuity point (Figure 6(a));
- (e) a discontinuity point and its preimage (Figure 6(b));
- (f) two discontinuity points (Figure 6(c)).

Note that if the map is piecewise monotone and has one discontinuity point, then the immediate basin of a chaotic attractor cannot be bounded by the discontinuity point (or its preimage). In fact, it is easy to show that in this case the discontinuity point necessarily belongs to the chaotic attractor.

For a *multiple-connected attractor* \mathcal{A} with k components (either a k -cycle, or a k -band chaotic attractor) the immediate basin $\mathcal{B}_0(\mathcal{A})$ consists of k intervals. In particular, if \mathcal{A} is an attracting k -cycle of map f , then its immediate basin consists of k intervals which are immediate basins of corresponding k fixed points of map f^k . To construct the total basin of attraction of \mathcal{A} the two steps described above can be carried out for the related fixed points of f^k (or, equivalently, for one of such fixed points, and then taking k images by f of the resulting set). If \mathcal{A} is a chaotic attractor consisting of k bands, then these bands

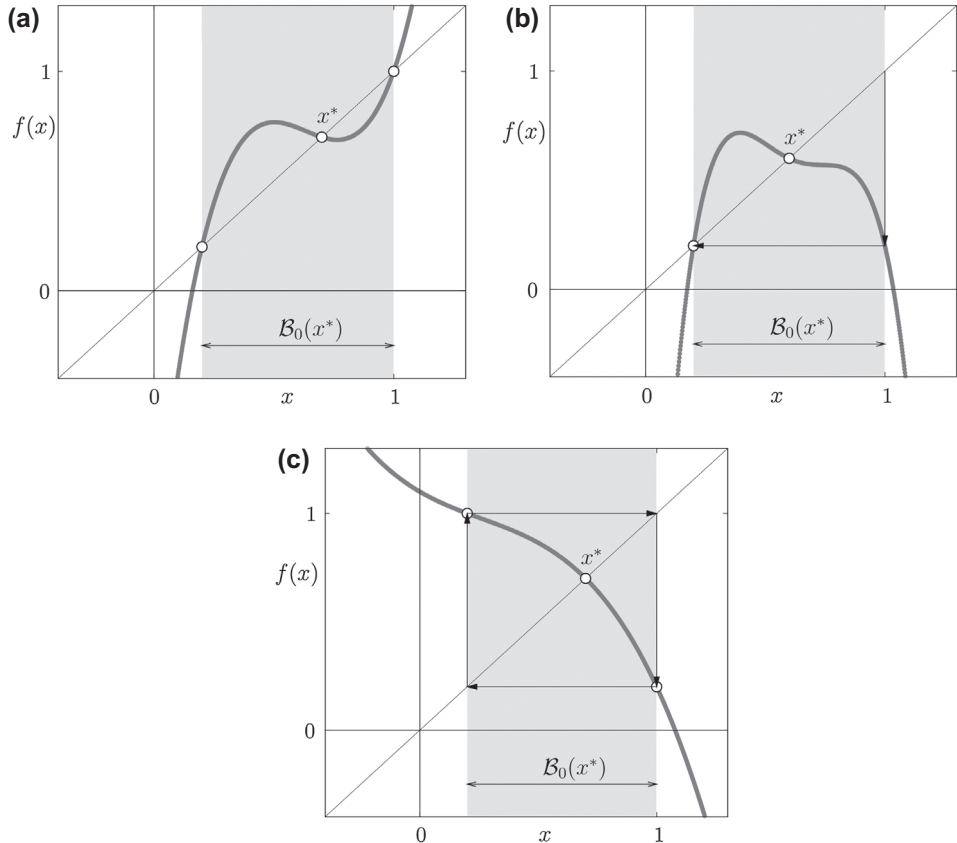


Figure 5. The immediate basin $\mathcal{B}_0(x^*)$ of an attracting fixed point x^* of a continuous map: $\mathcal{B}_0(x^*)$ is bounded by (a) two repelling fixed points; (b) a repelling fixed point and its rank-one preimage; (c) a repelling 2-cycle.

are necessarily cyclic if f is continuous, so that we can again consider the map f^k and the immediate basins of its k coexisting chaotic attractors. A k -band chaotic attractor of a discontinuous map may be acyclic (see Section 7.3), and in such a case its immediate basin has to be constructed directly, without considering f^k .

It may happen that the boundary of the immediate basin of an acyclic k -band chaotic attractor is constituted by points of several repelling cycles and their preimages. For example, the immediate basin of the 8-band chaotic attractor of map (2) shown in Figure 7 consists of 8 intervals bounded by points of the repelling 4-cycle $\{x_i^{(4)}\}_{i=0}^3$, points of the repelling 3-cycle $\{x_i^{(3)}\}_{i=0}^2$, as well as rank-one and rank-two preimages of the point $x_1^{(3)}$, namely, $f_R^{-1}(x_1^{(3)})$ and $f_L^{-1} \circ f_R^{-1}(x_1^{(3)})$.

It is known that the total basin $\mathcal{B}(\mathcal{A})$ of an attractor \mathcal{A} , even of such a simple invariant set as an attracting fixed point or a cycle, can have quite a complicated structure. The following cases can be distinguished:

- $\mathcal{B}_0(\mathcal{A})$ does not have any preimage other than itself, so that the total basin $\mathcal{B}(\mathcal{A})$ coincides with the immediate basin (see, e.g. Figure 5);
- $\mathcal{B}_0(\mathcal{A})$ has a finite number of preimages;

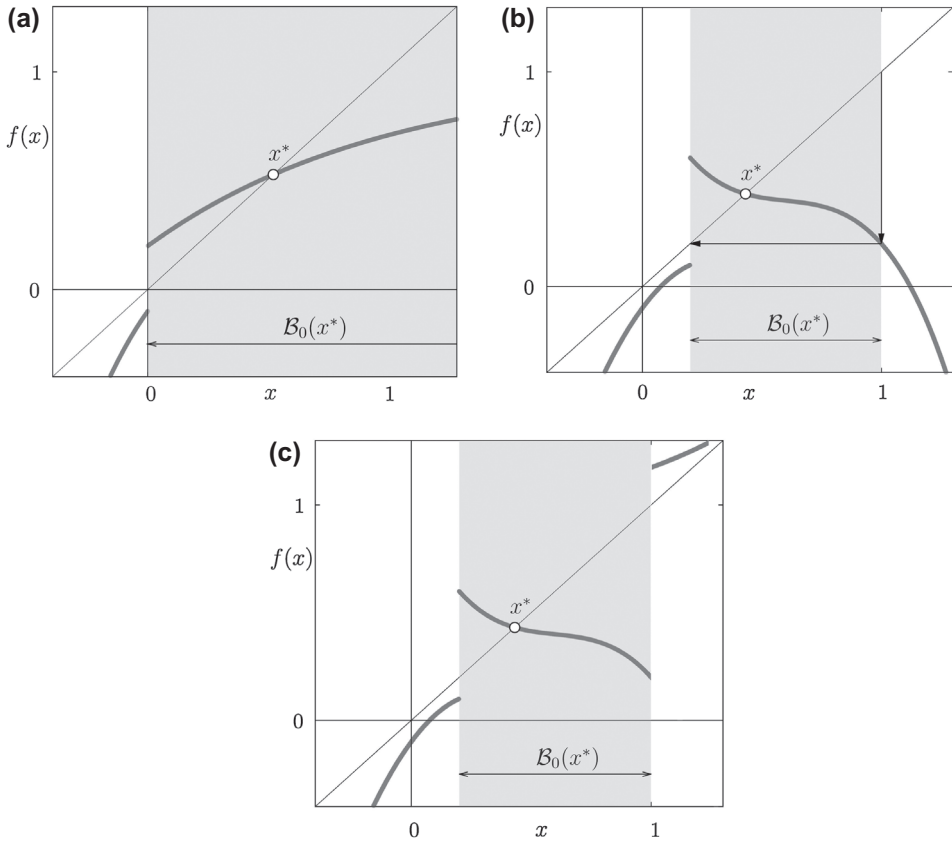


Figure 6. The immediate basin $\mathcal{B}_0(x^*)$ of an attracting fixed point x^* of a discontinuous map: $\mathcal{B}_0(x^*)$ is bounded by (a) the discontinuity point; (b) the discontinuity point and its rank-one preimage; (c) two discontinuity points.

- (c) $\mathcal{B}_0(\mathcal{A})$ has a countable number of preimages which accumulate under backward iterations to a finite number of repelling cycles;
- (d) $\mathcal{B}_0(\mathcal{A})$ has a countable number of preimages which accumulate under backward iterations to an infinite number of repelling cycles and constitute a set with a fractal structure.³

Note that in cases (c) and (d) divergent preimages may also exist.

The total basin of the chaotic attractor shown in Figure 7 consists of intervals separated from each other by the points of the 3- and 4-cycles and their preimages. It can be shown that these preimages converge in backward iterations to the repelling fixed point on the right side and to its rank-one preimage on the left side. Therefore, the total basin of the chaotic attractor is as in case (c) above.

As an example of case (d), we can consider the logistic map q given in (1), at a parameter value corresponding to an attracting 3-cycle. The points $\{x_i\}_{i=0}^2$ of this cycle represent fixed points for the third iterate q^3 . The immediate basins $\mathcal{B}_0(x_i)$, $i = 0, 1, 2$, of these fixed points are bounded by the repelling fixed points $\{x_i^u\}_{i=0}^2$ (corresponding to the repelling 3-cycle of q which appears in pair with the attracting 3-cycle at the fold bifurcation), and points

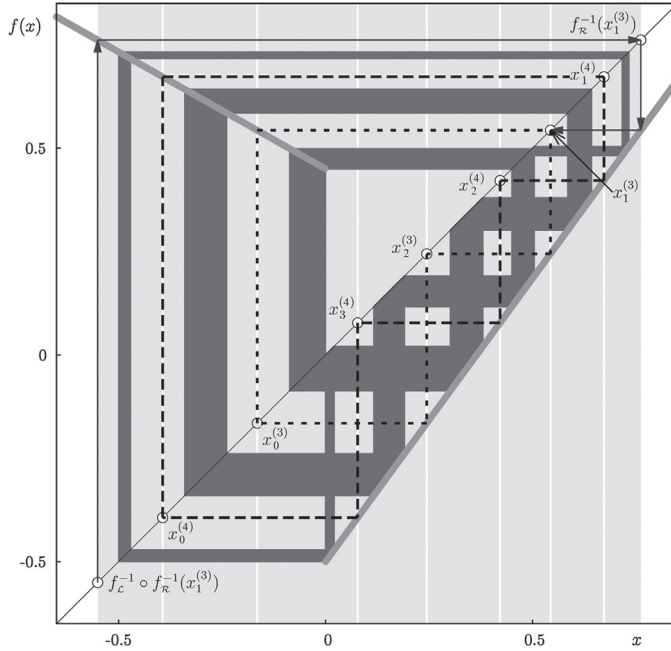


Figure 7. The immediate basin $\mathcal{B}_0(\mathcal{Q}_8)$ of an acyclic 8-band chaotic attractor \mathcal{Q}_8 of map (2) bounded by the points of repelling 4- and 3-cycles (shown with dashed lines) and two preimages of the point $x_1^{(3)}$. Parameters: $a_L = -0.566$, $a_R = 1.37$, $\mu_L = 0.45$, $\mu_R = -0.5$.

belonging to their rank-one preimages by q^3 . The immediate basin of the attracting 3-cycle is given by $\cup_{i=0}^2 \mathcal{B}_0(x_i)$. Considering map q^3 , for each attracting fixed points x_i we can obtain its total basin $\mathcal{B}(x_i)$, which is given by the union of all the preimages of $\mathcal{B}_0(x_i)$. The total basins of these three fixed points are separated from each other by a *chaotic repeller*, so that they have a fractal structure.

5. Repellers and other invariant sets

Let us now discuss non-attracting invariant sets of a 1D map $f : I \rightarrow I$ on an interval $I \subseteq \mathbb{R}$.

Definition 10: A closed invariant set Λ is called **repelling** if there exists a neighbourhood $\mathcal{U}(\Lambda)$ of Λ such that for any $x \in \mathcal{U}(\Lambda) \setminus \Lambda$ there exists k such that $f^k(x) \notin \mathcal{U}(\Lambda)$. A repelling set Λ with a dense orbit is called a **repeller**.

In other words, any initial point from the neighbourhood $\mathcal{U}(\Lambda)$ of a repelling set Λ is mapped outside $\mathcal{U}(\Lambda)$ in a finite number of iterations. Note that the initial points repelled from the neighbourhood $\mathcal{U}(\Lambda)$ may visit $\mathcal{U}(\Lambda)$ again, moreover, some of them may be mapped into Λ (as, e.g. in case of a homoclinic repelling fixed point or cycle).

5.1. Repelling cycles

The simplest case of a repeller is a repelling n -cycle $\mathcal{O} = \{x_i\}_{i=0}^{n-1}$, $n \geq 1$, of map f . Let us assume that either f is smooth, or, in case it is nonsmooth, no one point of the cycle

coincides with a kink or discontinuity point of f . Then the eigenvalue $\lambda(\mathcal{O})$ of \mathcal{O} is well defined, and a hyperbolic cycle \mathcal{O} with the eigenvalue $|\lambda(\mathcal{O})| > 1$ is repelling. Note that it is a sufficient but not necessary condition for a cycle to be repelling, as nonhyperbolic cycles may be repelling as well. For example, a nonhyperbolic cycle undergoing a subcritical flip or pitchfork bifurcation represents a repeller.

Consider a nonsmooth map f with a kink or discontinuity point $x = \hat{x}$, and a cycle \mathcal{O} of f which undergoes a border collision with, say, $x_0 = \hat{x}$. If \hat{x} is a kink point and it holds that $|(f^n)'(\hat{x}_-)| > 1, |(f^n)'(\hat{x}_+)| > 1$, then \mathcal{O} is locally repelling, while if \hat{x} is a discontinuity point, one can evaluate only one one-side derivative, and if it is larger than 1 in modulus, then \mathcal{O} is one-side (locally) repelling.

5.2. Chaotic repellers

Definition 11: A repelling set $\Lambda \subset I$ is called a **chaotic repeller** of a map $f : I \rightarrow I$, $I \subseteq \mathbb{R}$, if f is chaotic on Λ .

Among well-known examples of chaotic repellers we can mention the one of the logistic map (1) existing for $\alpha = 4$, which is the interval $I = [0, 1]$, i.e. $\Lambda = I$, or the set $\Lambda \subset I$ existing for $\alpha > 4$ which is homeomorphic to a Cantor set. For the skew tent map (4) similar chaotic repellors can be mentioned: at $a_R = \frac{a_L}{1-a_L}$ the interval $I = [f(\mu), \mu]$ is a chaotic repellor, and for $a_R < \frac{a_L}{1-a_L}$ (see Figure 2(c)) there exists a chaotic repellor $\Lambda \subset I$ homeomorphic to a Cantor set.

5.3. Critical attractors

There are particular invariant sets which are neither attracting, nor repelling. Besides a nonhyperbolic n -cycle at the moment of a fold or transcritical bifurcation (which are attractors in Milnor sense, see Definition 5, but not in the sense of Definition 4), it is worth describing the so-called *critical attractor*, also referred to as *Feigenbaum attractor*. Recall that critical attractors in general occur in maps with ‘smooth’ critical points at particular parameter values (called Feigenbaum accumulation points) related to the limit of a period-doubling cascade. An example of a critical attractor of the logistic map (1) is the set \mathcal{C} existing at $\alpha = \alpha_\infty$, where $\alpha_\infty \approx 3.56994567$ is the first Feigenbaum accumulation point. Set \mathcal{C} is a set of accumulation points for repelling cycles; it is homeomorphic to a Cantor set; it contains no periodic points; each point of \mathcal{C} is quasiperiodic and, thus, $\mathcal{C} = \omega(x)$ for any $x \in \mathcal{C}$; \mathcal{C} contains the critical point $f(1/2)$ and hence $\mathcal{C} = \omega(1/2)$ (for details see e.g. [72]). Obviously, the piecewise linear map (2) can not have a critical attractor.

It is worth to compare a critical attractor with a Cantor set attractor. Any point of both sets is quasiperiodic, they both are homeomorphic to a Cantor set and both are not chaotic because the property (2) of Definition 6 is not satisfied. However, *any* point from the neighbourhood of a Cantor set attractor is attracted to it (thus, it is an attractor according to Definition 4), while in any neighbourhood of a critical attractor there are points which are not attracted to it (repelling 2^k -cycles with arbitrary large k in the case of the first Feigenbaum attractor of the logistic map). This is the reason why a critical attractor is an attractor in Milnor sense but not an attractor according to Definition 4.

6. Homoclinic orbits and homoclinic bifurcations

Consider a map $f : I \rightarrow I$, $I \subseteq \mathbb{R}$, with a fixed point x^* . To define a homoclinic orbit of x^* we need first to recall the notions of stable and unstable invariant sets of a fixed point.

In short, the stable set of x^* is the set of points tending to x^* in forward iterations (by f), while the unstable set of x^* is the set of points tending to x^* in backward iterations (by f^{-1}). As we already mentioned, if the function f is noninvertible then its inverse f^{-1} has a number $k > 1$ of monotone branches, say, $f_1^{-1}, f_2^{-1}, \dots, f_k^{-1}$. In such a case the unstable set of x^* is defined by sequences of points $\{f_{j_i}^{-i}(x)\}_{i=1}^{\infty}$, tending to x^* as $i \rightarrow \infty$, where $j_i \in \{1, 2, \dots, k\}$. So,

Definition 12: The **stable** and **unstable sets** of a fixed point x^* of a map f are defined, respectively, as

$$W^s(x^*) = \left\{ x \mid \lim_{i \rightarrow \infty} f^i(x) = x^* \right\}, \quad W^u(x^*) = \left\{ x \neq x^* \mid \lim_{i \rightarrow \infty} f_{j_i}^{-i}(x) = x^* \right\}. \quad (6)$$

If x^* is an *attracting* fixed point, then its stable set coincides with the basin of attraction $\mathcal{B}(x^*)$, and its unstable set is empty. If x^* is a *repelling* fixed point, then taking an ϵ -neighbourhood of x^* (called the *local unstable set* of x^*) and all its images, we get the unstable set of x^* , while its stable set is not empty only if the map is noninvertible and the fixed point x^* has preimages different from itself. In such a case the stable set is the union of all the preimages of x^* . It is worth to note that in general the set W^s of a repelling fixed point is at most a countable set of points,⁴ whereas the set W^u is a set of intervals, while for an attracting fixed point the set W^u is empty and W^s is a set of intervals.

As an example, Figure 8 shows the stable and unstable sets of the fixed point \mathcal{O}_R of the logistic map (1): the unstable set $W^u(\mathcal{O}_R)$ is empty for $\alpha \leq 3$, since the fixed point is attracting. For $\alpha > 3$, the set $W^u(\mathcal{O}_R)$ is given by the complete absorbing interval $J = [q(c), c]$. Regarding the stable set $W^s(\mathcal{O}_R)$, the situations is more sophisticated. For $\alpha \leq 3$ it covers the interval $(0, 1)$, which is the total basin of attraction of \mathcal{O}_R . As the fixed point \mathcal{O}_R becomes repelling, its stable set becomes a set of points (preimages of \mathcal{O}_R). For $\alpha < \bar{\alpha}_1$ with $\bar{\alpha}_1 \approx 3.67834$ (see Figure 8), these preimages form two sequences converging monotonously in backward iterations to $x = 0$ and to $x = 1$ (that is, to the repelling fixed point \mathcal{O}_L and its unique preimage). Using the two branches of the inverse function q^{-1} of the logistic map, given by

$$q_1^{-1}(x) = \frac{1}{2} \left(1 - \sqrt{1 - \frac{4x}{\alpha}} \right) \quad \text{and} \quad q_2^{-1}(x) = \frac{1}{2} \left(1 + \sqrt{1 - \frac{4x}{\alpha}} \right) \quad (7)$$

one can easily see that these two sequences are given by

$$\{q_1^{-i}(\mathcal{O}_R) \mid i > 0\} \quad \text{and} \quad \{q_2^{-i}(q_1^{-i}(\mathcal{O}_R)) \mid i > 0\}. \quad (8)$$

At the parameter value $\alpha = \bar{\alpha}_1$ corresponding to the first homoclinic bifurcation of \mathcal{O}_R the situation changes significantly.⁵ As one can see in Figure 8, an ‘explosion’ of preimages is observed at this point. For increasing α these preimages persist and additionally infinitely many new preimages appear. The difference between the cases $\alpha < \bar{\alpha}_1$ and $\alpha > \bar{\alpha}_1$ is illustrated in Figure 9. For $\alpha < \bar{\alpha}_1$ (see Figure 9(a)) the rank-one preimage $q_1^{-1}(\mathcal{O}_R)$

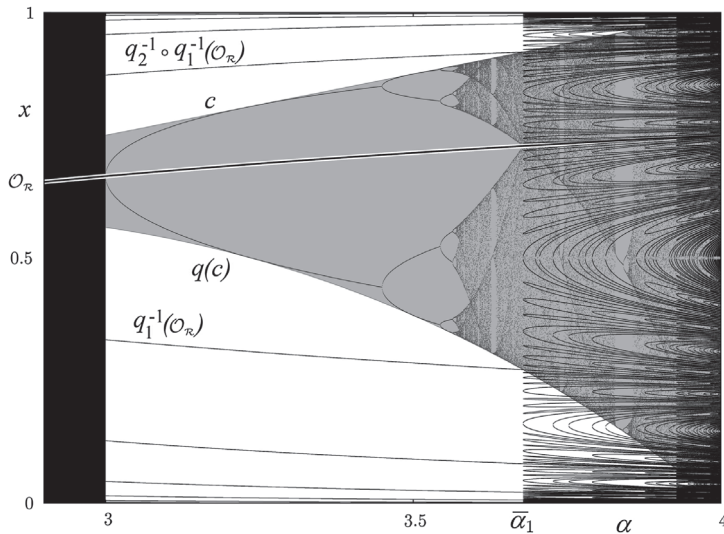


Figure 8. The unstable set $W^u(O_R)$ of the fixed point O_R of the logistic map is shown in grey, the stable set $W^s(O_R)$ is shown black. The 1D bifurcation diagram is also shown.

is located outside the absorbing interval $J = [q(c), c]$. It has two preimages $q_1^{-2}(O_R)$ and $q_2^{-1}(q_1^{-1}(O_R))$, among which $q_2^{-1}(q_1^{-1}(O_R))$ cannot have any preimage because it is located in the Z_0 region. The same is also true for all further preimages $q_1^{-i}(O_R)$ for any $i > 1$, and hence no preimage of O_R can exist which is different from those given by Equation (8). Then, at $\alpha = \bar{\alpha}_1$, the rank-one preimage $q_1^{-1}(O_R)$ collides with the left boundary of the interval J , the rank-two preimage $q_2^{-1}(q_1^{-1}(O_R))$ collides with its right boundary (see Figure 9(b)) and then infinitely many further preimages exist in J . For $\alpha > \bar{\alpha}_1$ these preimages enter inside the interval J (see Figure 9(c)). As a consequence, infinitely many new preimages of $q_2^{-1}(q_1^{-1}(O_R))$ appear (because now this point belongs to the Z_2 region) both inside and outside J , as can clearly be seen in Figure 8 where the preimages of O_R are shown up to the rank-10.

As we have seen in the above example, stable and unstable sets of a repelling fixed point x^* may intersect, i.e. a point p belonging to both of them may exist, which means

$$p \in W^s(x^*) \cap W^u(x^*). \quad (9)$$

Such a point p is called a *homoclinic point* of x^* .

Note that the sequence of images of a homoclinic point p and a suitable sequence of preimages of p consist of points which are also homoclinic, and furthermore, both these sequences converge to x^* . The union of these sequences is called a *homoclinic orbit* of x^* :

$$\mathcal{O}(x^*) = \{\dots, p_{-2}, p_{-1}, p_0, p_1, p_2, \dots, p_m\}, \quad (10)$$

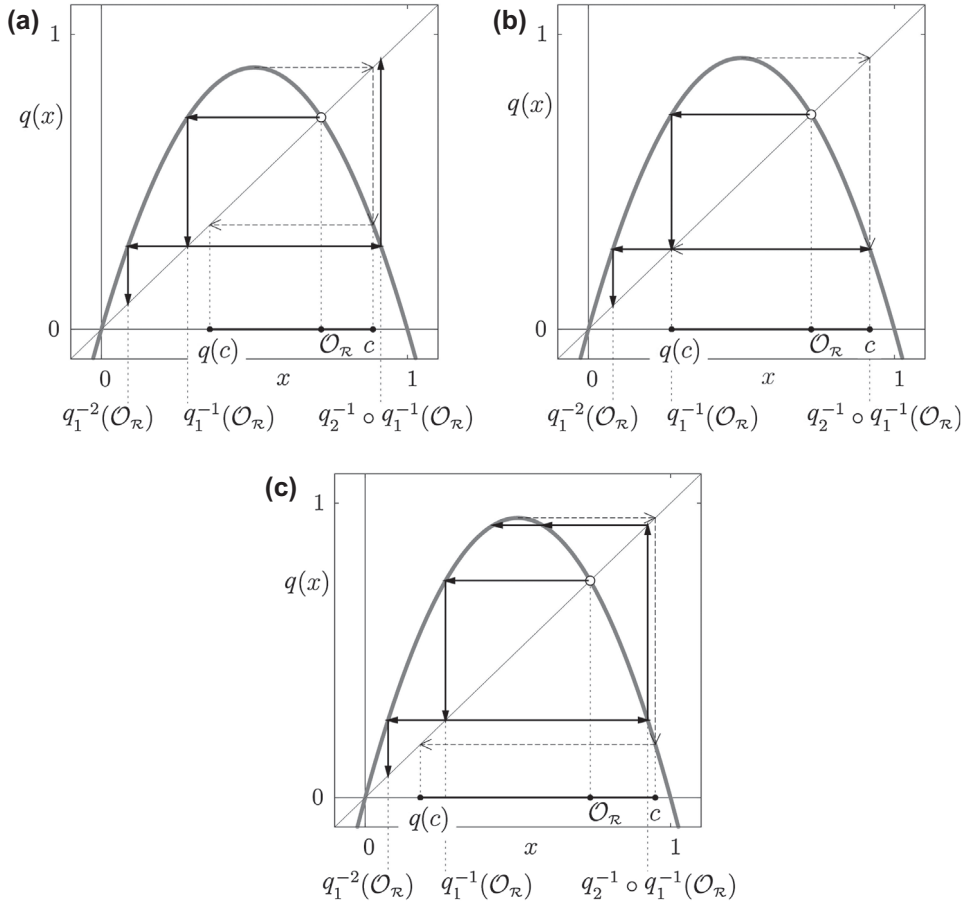


Figure 9. In (a), the rank-one preimage $q_1^{-1}(\mathcal{O}_R)$ of the fixed point \mathcal{O}_R of the logistic map is located outside the absorbing interval $J = [q(c), c]$, in (b) it contacts J (the first homoclinic bifurcation of \mathcal{O}_R occurs), and in (c) it enters inside J . Parameters: $\alpha = 3.55$ (a); $\alpha = \bar{\alpha}_1 \approx 3.678573511$ (b); $\alpha = 3.8$ (c).

where

$$p_0 \equiv p; \quad (11a)$$

$$p_{i+1} = f(p_i) \text{ for } i \leq m-1; \quad (11b)$$

$$p_m = x^* \text{ and } \lim_{i \rightarrow -\infty} p_i = x^*. \quad (11c)$$

It is evident from this definition that a homoclinic orbit is convergent in backward iterations to the fixed point x^* and, thus, every homoclinic orbit in backward iterations ends with preimages obtained with the same function, namely, the local inverse in the fixed point (that is, the function f_j^{-1} for which $f_j^{-1}(x^*) = x^*$). So, given any homoclinic orbit, we can characterize it with a homoclinic point p of the orbit *belonging to a neighbourhood* of the fixed point, so that the preimages of p are taken only with the local inverse. Hence, in Equation (10) we have

$$p_0 = p; \quad p_i = f^i(p) \text{ for } 1 \leq i \leq m; \quad \text{and} \quad p_{-i} = f_j^{-i}(p) \text{ for } i \geq 1. \quad (12)$$

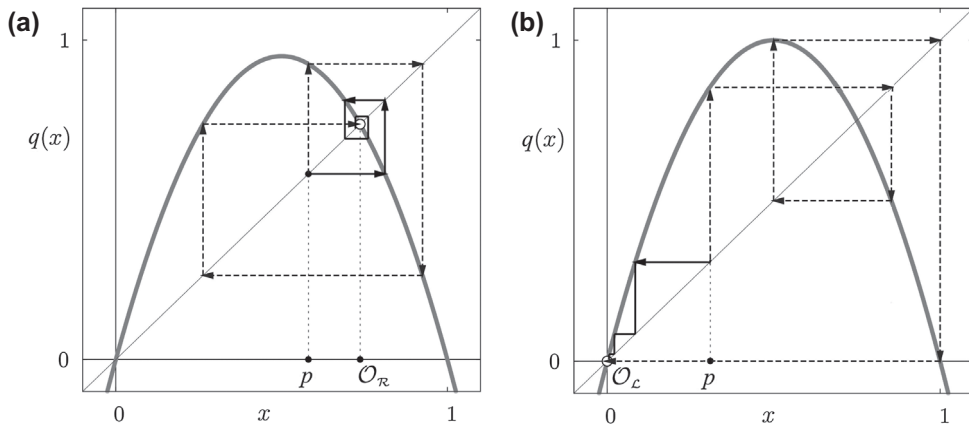


Figure 10. Homoclinic orbits of the repelling fixed points \mathcal{O}_R (a) and \mathcal{O}_L (b) of the logistic map. Dashed lines show forward iterations, solid lines backward iterations of the homoclinic point p . Parameter values: $\alpha = 3.8$ (a); $\alpha = 4.0$ (b).

As an example in Figure 10(a) a homoclinic orbit of the repelling fixed point \mathcal{O}_R of the logistic map is shown. In this figure, the homoclinic point p with $q^3(p) = \mathcal{O}_R$ is marked. It can easily be seen how the homoclinic orbit converges to the fixed point \mathcal{O}_R both in forward and backward iterations. It is also evident that from the two inverse functions of the logistic map q_1^{-1} and q_2^{-1} , given by Equation (7), the local inverse at the fixed point \mathcal{O}_R is q_2^{-1} . Similarly, Figure 10(b) shows a homoclinic orbit of the repelling fixed point \mathcal{O}_L of the logistic map and the homoclinic point p with $q^4(p) = \mathcal{O}_L$. The local inverse at the fixed point \mathcal{O}_L is q_1^{-1} .

A point p belongs to a *heteroclinic orbit* from a fixed point x^{**} of a noninvertible map f to some other fixed point x^* of f if p is mapped into x^* in a finite number of forward iterations and a suitable sequence of preimages of p approaches x^{**} in backward iterations. A *heteroclinic connection* between two fixed points x^* and x^{**} of a map f is the union of two heteroclinic orbits, from x^* to x^{**} and from x^{**} to x^* . Obviously, heteroclinic connections may exist not only between fixed points, but also between fixed points and cycles, or between two cycles. Recall that heteroclinic connections have the same properties as homoclinic orbits.

6.1. Homoclinic bifurcations

The existence of a homoclinic orbit of a fixed point or cycle plays a significant role for the dynamics of a map, as it can be shown (see e.g. [54,55]) that in any neighbourhood of a nondegenerate homoclinic orbit there exists an invariant set on which the map is chaotic.

The occurrence of the first homoclinic orbit is closely related to the notion of *degenerate homoclinic orbit* introduced to investigate this bifurcation in smooth dynamical systems. In [34] a *critical homoclinic orbit* is defined, and it is shown that in 1D maps only critical homoclinic orbits are responsible for the first homoclinic bifurcation as well as for the other homoclinic explosions, and this occurs not only in smooth but also in piecewise smooth maps, both in continuous and discontinuous ones. Below we summarize the main definitions and some results presented in [34], which are related to 1D maps.

Consider a 1D map $f : I \rightarrow I$, $I \subseteq \mathbb{R}$. To simplify the exposition we limit our reasoning to a fixed point x^* of map f . Recall first the following:

Definition 13: A fixed point x^* is called **expanding** if f is continuous in x^* and a neighbourhood U of x^* exists such that for any $x \in U \setminus x^*$ an integer n_x exists for which $f^{n_x}(x) \notin U$, and a local inverse f_1^{-1} satisfies $\cap_{n \geq 0} f_1^{-n}(U) = x^*$.

Here we have not made use of the derivative of f at x^* , as in fact it is possible to characterize the homoclinic bifurcations independently on the smoothness of the function in the homoclinic points. It is clear, however, that if f is smooth in x^* then a sufficient condition for the fixed point x^* to be expanding is $|\lambda(x^*)| > 1$, as in this case the local inverse behaves as a contraction, that is, x^* has to be repelling.

So, in the following, considering a neighbourhood U of a repelling fixed point x^* , it is understood that it is a neighbourhood as in Definition 13, and we also say that f is *locally invertible* in x^* with local inverse f_1^{-1} .

Given a repelling fixed point x^* of map f , any point in a neighbourhood U of x^* is repelled away (thus no local stable set can exist), but when f is noninvertible then the trajectory of a point may come back to U again. This occurs when x^* is homoclinic, that is, when *arbitrarily close to x^* preimages of the fixed point can be found*. When this occurs the fixed point is called, after Marotto (see [54]) a *snap-back repeller* (SBR). Recall that in [54] the definition of SBR is given for a differentiable map $f : \mathbb{R}^n \rightarrow \mathbb{R}^n$, under the assumption that all the eigenvalues of the Jacobian $J_f(x^*)$ exceed 1 in modulus, and $\det(J_f(x_j)) \neq 0$ in all the homoclinic points, called nondegenerate homoclinic orbit. We use a different definition of a SBR according to which the fixed point (or a homoclinic point) may be a point of nonsmoothness of f :

Definition 14: Let x^* be a repelling fixed point of $f : I \rightarrow I$, $I \subseteq \mathbb{R}$. The fixed point x^* is called a **snap-back repeller** if there exists a point $x_0 \in U \setminus x^*$ such that $f^m(x_0) = x^*$ for a suitable integer m . The orbit $\mathcal{O}(x^*)$ given by

$$\mathcal{O}(x^*) = \left\{ x^* \leftarrow \dots, f_1^{-n}(x_0), \dots, f_1^{-1}(x_0), x_0, x_1, \dots, x_m = x^* \right\} \quad (13)$$

is the related homoclinic orbit, where $x_i = f^i(x_0)$, $i = 1, \dots, m$.

Smooth maps are considered also in [27], and a nondegenerate homoclinic orbit is defined as follows:

Definition 15: A homoclinic orbit $\mathcal{O}(x^*)$ of an expanding fixed point x^* of a smooth map $f : X \rightarrow X$, $X \subseteq \mathbb{R}^n$ is called **nondegenerate** if $\det(J_f(x_j)) \neq 0$ in all the points x_j of the orbit.

In [54] (as well as in [27]) for a smooth map the following result is proved:

Theorem 1: If a smooth map $f : X \rightarrow X$, $X \subseteq \mathbb{R}^n$, has an SBR x^* such that all the eigenvalues of $J_f(x^*)$ exceed 1 in modulus, and $\mathcal{O}(x^*)$ is a nondegenerate homoclinic orbit, then in any neighbourhood of $\mathcal{O}(x^*)$ there exists an invariant set on which f is chaotic.

Note that from Theorem 1 nothing can be deduced about the bifurcation which leads an expanding fixed point to become an SBR (called *SBR bifurcation*), as well as other homoclinic bifurcations leading to infinitely many new nondegenerate homoclinic orbits, called *Ω -explosions*. It is clear that to identify such bifurcations one must look for homoclinic orbits which are *degenerate*, i.e. not satisfying the condition of nondegeneracy. There

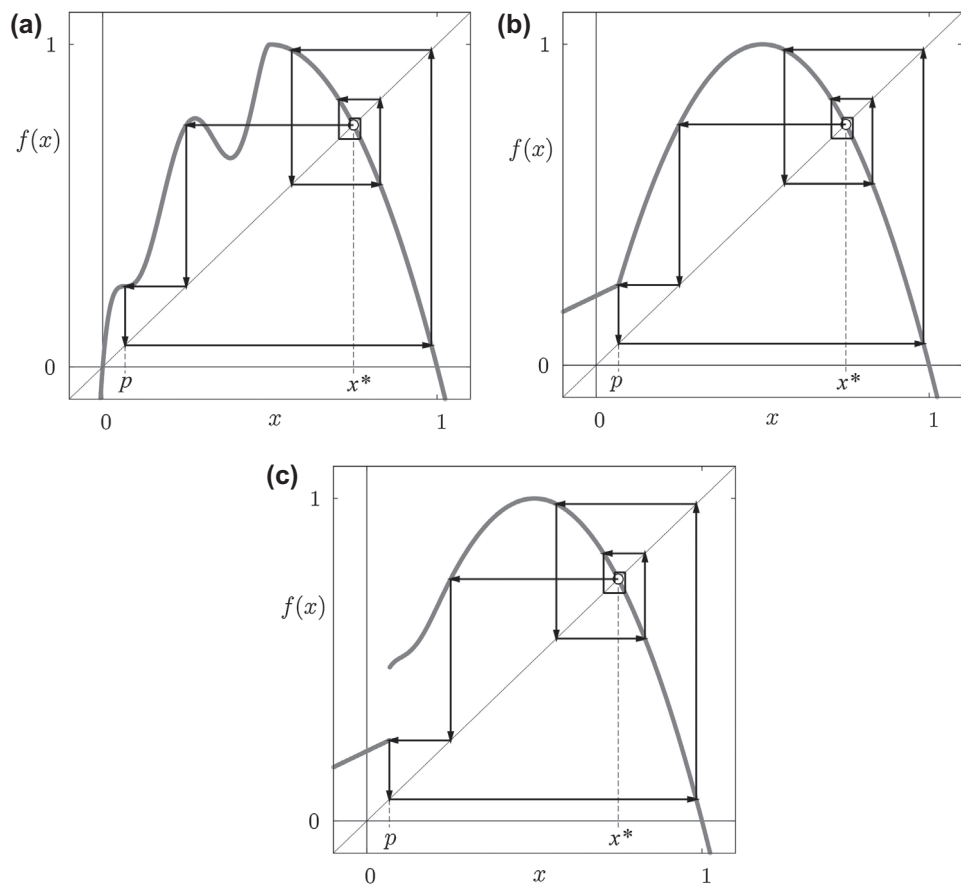


Figure 11. Degenerate homoclinic orbits of the repelling fixed point x^* : (a) f has a vanishing derivative at the point p (inflection point); (b) f is continuous but nondifferentiable at the point p ; (c) f is discontinuous at the point p .

are, however, several kinds of degeneracy, both for smooth and piecewise smooth maps, and the relevant ones are only the degenerate homoclinic orbits which are structurally unstable (with respect to the existence of the homoclinic orbit). For example, a homoclinic orbit including a point p such that $f'(p) = 0$, is degenerate but not necessarily related to a homoclinic bifurcation. Under suitable assumptions given below it may also be a persistent (under parameter perturbation) homoclinic orbit, not involved in any Ω -explosion. For example, if a point p of the degenerate homoclinic orbit of f is a point of local extremum of f then this may indicate a bifurcation, but not when a point p is an inflection point. It can be seen that in the last case the homoclinic orbit is persistent, as in the example shown in Figure 11(a). For piecewise smooth maps the derivative may be undefined in a homoclinic point p , but this does not necessarily mean that the orbit is structurally unstable, as shown in Figure 11(b) where the homoclinic orbit is persistent as well. The function may be discontinuous in a homoclinic point p (see Figure 11(c)), and here the homoclinic orbit is necessarily not persistent (if the preimage of the fixed point moves on its right side the homoclinic orbit disappears, differently from the case when it moves on the left).

Indeed, if a point p of a homoclinic orbit is a point of nondifferentiability or it is such that $f'(p) = 0$, then Theorem 1 cannot be applied. However, in the particular situations shown in Figure 11(a) and (b), Theorem 2 given below applies and states the existence of chaos. In fact, what matters in order to classify the first homoclinic orbit of an expanding fixed point x^* , as well as to characterize further homoclinic explosions, is a homoclinic orbit for which the local invertibility is lost in some homoclinic point (thus, such a homoclinic orbit is not persistent under parameter perturbation). The important property of a structurally stable homoclinic orbit $\mathcal{O}(x^*)$ is that in each point x_k of this orbit *the function is continuous and locally monotone (either increasing or decreasing)* and thus locally invertible in a neighbourhood of each point of the homoclinic orbit. That is, we say that f is *locally invertible* in a point $x_k \in \mathcal{O}(x^*)$ if f is continuous at x_k , and a neighbourhood V_{x_k} of x_k exists in which f is invertible, that means one-to-one in V_{x_k} and onto $f(V_{x_k})$. This leads us to the following definition of a *noncritical homoclinic orbit*:

Definition 16: A homoclinic orbit $\mathcal{O}(x^*)$ of a repelling fixed point x^* of a map $f : I \rightarrow I$, $I \subseteq \mathbb{R}$, is called **noncritical** if f is locally invertible in each point of $\mathcal{O}(x^*)$.

A homoclinic orbit $\mathcal{O}(x^*)$ is *critical* if it includes a critical point (which is either an extremum associated with a continuous branch off, or the limit value off at a discontinuity point), or it is unbounded. Note that we do not write that the critical homoclinic orbit of a discontinuous map includes a discontinuity point, in order to emphasize that it does not matter how the function is defined at the discontinuity point, any one of the limit values may be involved in a critical homoclinic orbit.

The existence of a noncritical homoclinic orbit is important due to the following Theorem 2 ([34]) which generalizes Theorem 1 (namely, the homoclinic orbit is required to be noncritical instead of nondegenerate⁶):

Theorem 2: Let f be a piecewise smooth noninvertible map, $f : I \rightarrow I$, $I \subseteq \mathbb{R}$. Let x^* be a repelling fixed point of f and $\mathcal{O}(x^*)$ a noncritical homoclinic orbit of x^* . Then in any neighbourhood of $\mathcal{O}(x^*)$ there exists an invariant Cantor set Λ on which f is chaotic.

The property often used to prove that the map is chaotic on some set (in a phase space of any dimension), is the existence of two disjoint compact sets, say U_0 and U_1 , such that

$$f^k(U_0) \supset U_0 \cup U_1 \quad \text{and} \quad f^k(U_1) \supset U_0 \cup U_1 \quad (14)$$

for a suitable k . In the 1D case a map f with such a property is called *strictly turbulent* following [20].

As noted above, the homoclinic orbits which are particular are only the critical homoclinic orbits according to our definition, and they are the candidates to characterize the homoclinic bifurcations (not only the first one but any other as well).

Theorem 2 characterizes structurally stable homoclinic orbits, considering noncritical homoclinic orbits of x^* , and its proof does not depend on the structure of the set I . Meanwhile, a critical homoclinic orbit also depends on the definition of f in I . In fact, the dynamic behaviour in a neighbourhood of a critical homoclinic orbit cannot be uniquely characterized as chaotic or not a priori. As we show below, in the neighbourhood of a critical homoclinic orbit the dynamic behaviour depends on the particular system. Both in smooth and piecewise smooth maps, in any neighbourhood of a critical homoclinic orbit a *chaotic set may exist or may not exist*.

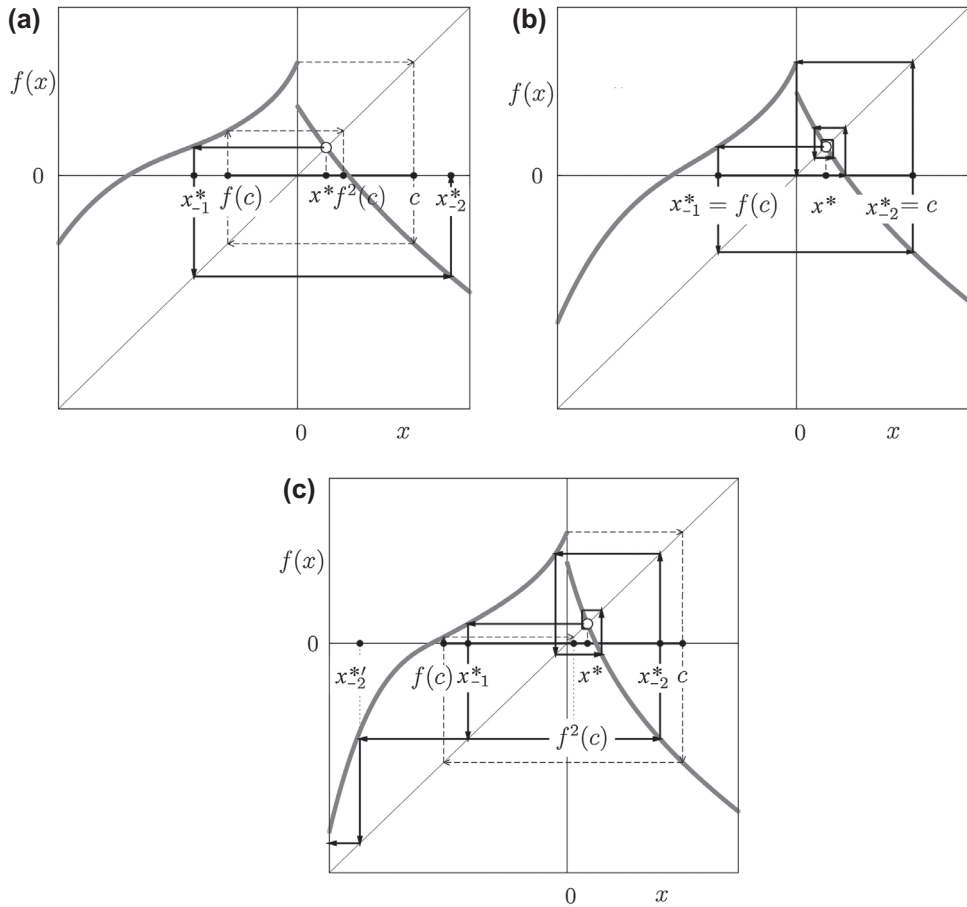


Figure 12. Homoclinic bifurcation of the fixed point x^* : (a) There is no homoclinic orbit of x^* ; (b) All the orbits homoclinic to x^* are critical; (c) There are noncritical homoclinic orbits of x^* .

Figure 12 shows a discontinuous map f with two branches f_L and f_R , in which we have the value $f_L(0)$, denoted by c , as a maximum, and the map is invariant in an absorbing interval $J = [f(c), c]$. As long as $f^2(c) > x^*$ (Figure 12(a)) the fixed point x^* has no homoclinic orbit. A neighbourhood of x^* exists which cannot include other periodic points: Indeed, it can be easily seen in Figure 12(a) that periodic points cannot exist in the interval $[f^3(c), f^2(c)]$. Therefore, no invariant chaotic set can include x^* . This is true as long as the unique rank-one preimage of x^* different from x^* is outside the interval J (as in Figure 12(a)). For $f^2(c) = x^*$, or $f(c) = x_{-1}^*$ (Figure 12(b)), the fixed point x^* has a critical homoclinic orbit and in any neighbourhood of this critical homoclinic orbit *there exists an invariant set in which the map is chaotic*. For $f^2(c) < x^*$ (Figure 12(c)) the fixed point x^* has infinitely many noncritical and nondegenerate homoclinic orbits which are persistent under parameter perturbation.

When a map is investigated as a function of some parameters, one can observe the first SBR bifurcation followed by infinitely many further homoclinic explosions, and all of them are associated with critical homoclinic orbits. In fact, whenever a preimage of the fixed point enters from outside the invariant absorbing interval to inside, a new critical homoclinic

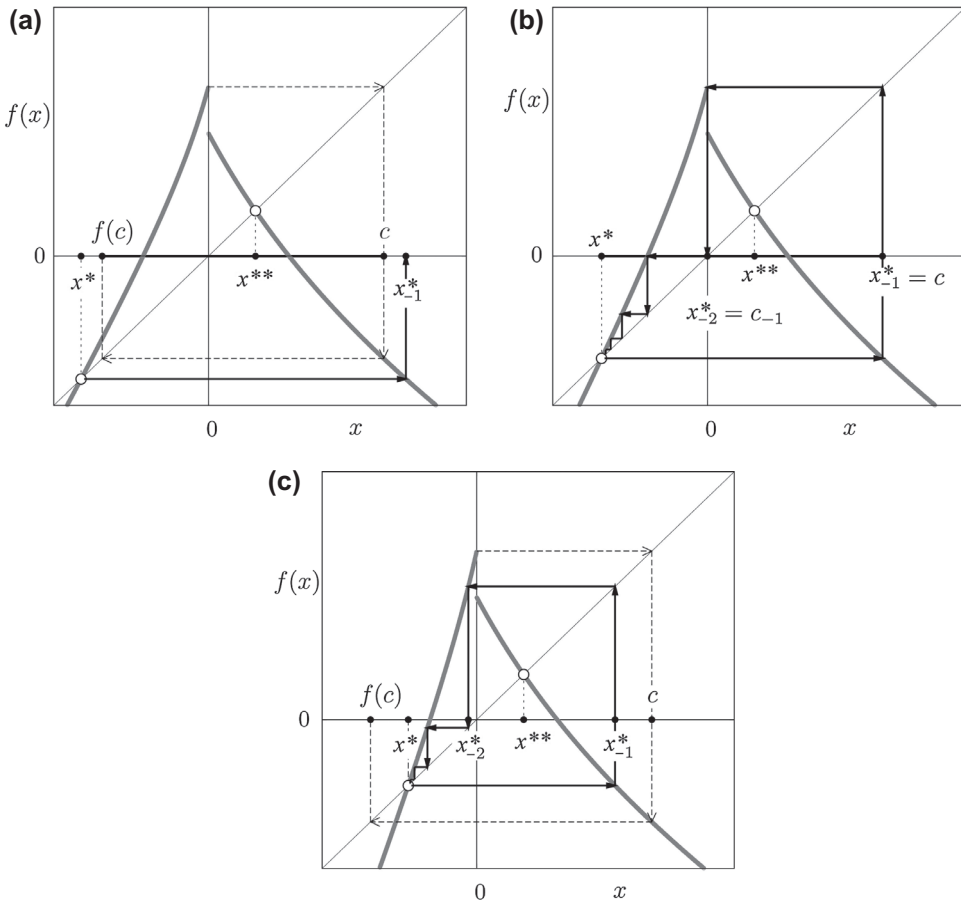


Figure 13. Homoclinic bifurcation of the fixed point x^* , $x^* \notin J = [f(c), c]$: (a) There are no homoclinic orbits of x^* ; J is an invariant absorbing interval; (b) All the orbits homoclinic to x^* are critical; J is invariant but not attracting; (c) There are noncritical homoclinic orbits of x^* belonging to a chaotic repeller; J is no longer invariant.

orbit appears. For example, in Figure 12(c) the point x_{-2}' is a rank-2 preimage of x^* outside the interval J , and if the parameters are changed so that $f(c) = x_{-2}'$, then infinitely many new critical homoclinic orbits appear (followed by infinitely many other noncritical and nondegenerate homoclinic orbits), again associated with chaotic behaviours and with an explosion of other repelling cycles.

Similarly, Figure 13 shows the first SBR bifurcation of a fixed point x^* , but now before the bifurcation (see Figure 13(a)) the fixed point does not belong to an invariant absorbing interval $J = [f(c), c]$, and the basin of attraction of J is confined by the point x^* and its rank-1 preimage. The difference is that in the example shown in Figure 12(c) the nondegenerate homoclinic orbits, appearing due to the critical homoclinic orbit, belong to a chaotic set inside the *invariant absorbing interval I*, while in the example shown in Figure 13(c) these belong only to a chaotic repeller (in fact, the interval $J = [f(c), c]$ in Figure 13(b) is invariant but not attracting, and no longer invariant in Figure 13(c)). Note that the other fixed point x^{**} of the map shown in Figure 13, belonging to J , is homoclinic, and

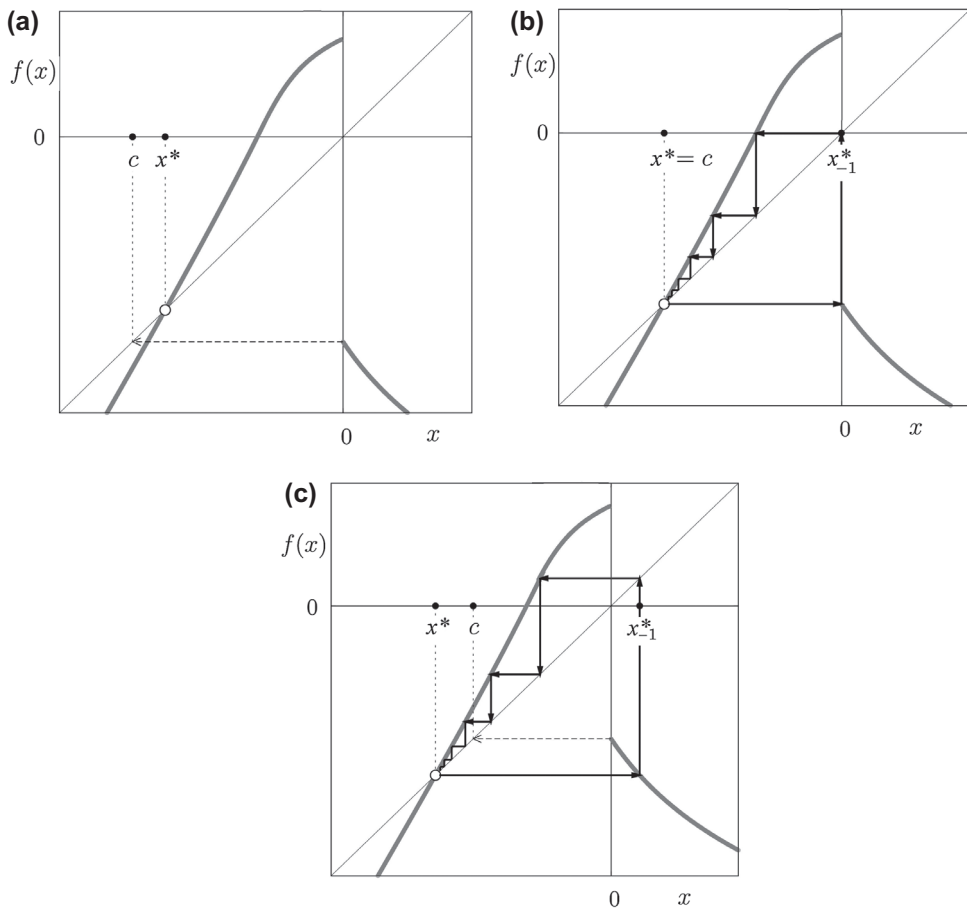


Figure 14. Homoclinic bifurcation of the fixed point x^* : (a) There are no homoclinic orbits of the fixed point x^* ; (b) There exists a unique critical homoclinic orbit of x^* ; (c) There are noncritical homoclinic orbits of x^* belonging to a chaotic repeller.

as the parameters are changed from Figure 13(a) to Figure 13(b) infinitely many critical homoclinic orbits of x^{**} also appear.

A critical homoclinic orbit, however, is not necessarily associated with a chaotic invariant set. Figure 14 shows a discontinuous map in which we vary the value $f_R(0)$ denoted by c . For $c < x^*$ (Figure 14(a)) the expanding fixed point x^* has no homoclinic orbit. For $c = x^*$ (Figure 14(b)) the fixed point x^* has a *unique critical homoclinic orbit* (SBR bifurcation of x^*)

but nevertheless in any neighbourhood of the critical homoclinic orbit *we cannot find an invariant set in which the map is chaotic*. In fact, in Figure 14(b) the repelling fixed point x^* and this critical homoclinic orbit are the unique nondivergent trajectories. For $c > x^*$ (Figure 14(c)) we have an explosion of infinitely many different noncritical homoclinic orbits of x^* (persistent under parameter perturbation) and a chaotic repeller exists.

As already mentioned, to prove the existence of chaos associated with a critical homoclinic orbit, to which the theorems given above cannot be applied, it is enough to show that we can find two disjoint intervals, U_0 and U_1 , such that (14) holds. The fact that this does not always occur has been demonstrated by the example shown in Figure 14(b).

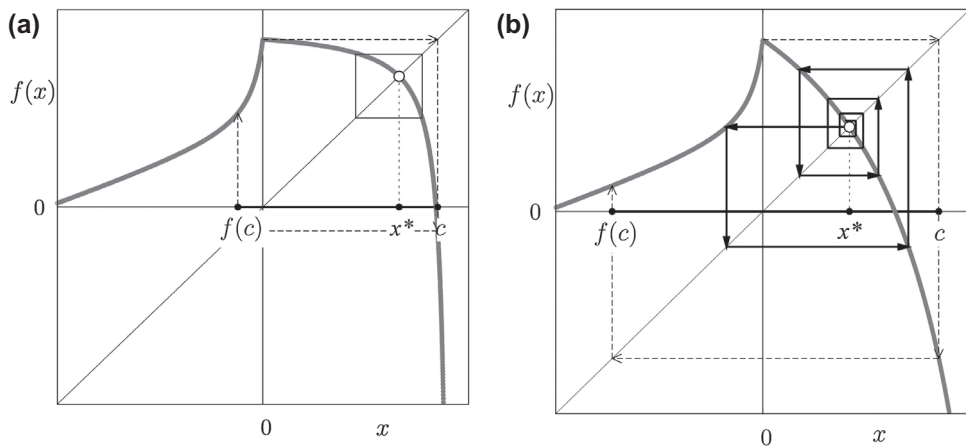


Figure 15. Before the flip bifurcation the fixed point x^* is attracting (a). After the subcritical flip bifurcation it is repelling and homoclinic (b).

So far we have characterized the homoclinic bifurcations which lead a repelling fixed point x^* to become SBR. Recall also that if $\lambda(x^*) < -1$ then SBR bifurcation of x^* leads to homoclinic points on both sides of x^* , while if $\lambda(x^*) > 1$ then its SBR bifurcation in general leads to homoclinic points on one side only. Thus, it may occur, afterwards, that another Ω -explosion creates homoclinic points on the other side. In this case we may distinguish between two SBR bifurcations associated with the two sides of x^* (as both are global bifurcations which may have relevant dynamic effects).

However, it is worth mentioning that the appearance of noncritical and nondegenerate homoclinic orbits of a fixed point may also occur via different kinds of bifurcations, both local and global. For example, an attracting fixed point or cycle may become repelling and homoclinic due to a flip bifurcation, as shown in Figure 15. In this example, the fixed point x^* which is attracting in Figure 15(a), undergoes a subcritical flip bifurcation and immediately after the bifurcation infinitely many nondegenerate and noncritical homoclinic orbits appear, as can be seen in Figure 15(b).

7. Properties of chaotic attractors

7.1. Boundaries of chaotic attractors

When dealing with chaotic attractors, it is often important to determine their boundaries. In particular, it is necessary for the calculation of the parameter values corresponding to such transformations of chaotic attractors as merging, expansion and final bifurcations (see [8] for details). For chaotic attractors of 1D maps the boundaries can easily be obtained due to the following:

Proposition 1: *The boundaries of an n -band chaotic attractor \mathcal{A} , $n \geq 1$, of a 1D map are given by critical points and their images.*

For the piecewise linear map (2) and in general for 1D piecewise monotone maps with one border point, this proposition implies that all the boundaries are determined by the images of the single border point. Hereby, for an n -band chaotic attractor of a continuous

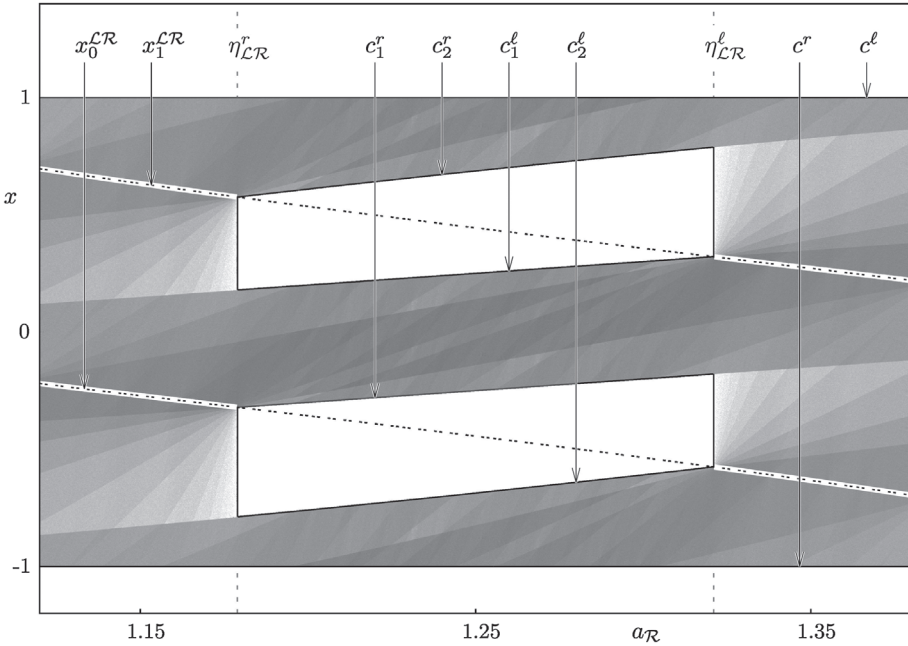


Figure 16. One- and three-band chaotic attractors of map (2) and their boundaries determined by critical points. Parameters: $\mu_L = 1$, $\mu_R = -1$, $a_L = 2.5 - a_R$.

map f with one critical point $x = c$ the boundaries are determined by this critical point and its images, that is, by the sequence of points $\{c_i\}_{i=0}^{2n-1}$ where $c_0 \equiv c$ and $c_i = f^i(c)$. For a 1D map f with monotone branches f_L and f_R and one discontinuity point $x = 0$, an n -band chaotic attractor is bounded by points which belong to at least one of the sequences, $\{c_i^\ell\}_{i=0}^{2n-1}$ and $\{c_i^r\}_{i=0}^{2n-1}$, or to both of them, where $c_0^\ell \equiv c^\ell = f_L(0)$, $c_i^\ell = f^i(c^\ell)$, $c_0^r \equiv c^r = f_R(0)$ and $c_i^r = f^i(c^r)$.

As an example, Figure 16 shows one- and three-band attractors of the discontinuous map (2). Their boundaries are defined by two critical points, $c^\ell = f_L(0) = \mu_L$ and $c^r = f_R(0) = \mu_R$, as well as their images, c_i^ℓ and c_i^r , $i = 1, 2$.

Proposition 1 can be proved in a few steps. Let us consider a closed invariant attracting set \mathcal{A} of a 1D map $f : I \rightarrow I$, $I \subseteq \mathbb{R}$. Recall that the invariance of \mathcal{A} means $f(\mathcal{A}) = \mathcal{A}$ and that the attractiveness of \mathcal{A} implies the existence on a neighbourhood $\mathcal{U}(\mathcal{A})$ such that for any $x \in \mathcal{U}(\mathcal{A})$ the ω -limit set of x belongs to \mathcal{A} . From the invariance of \mathcal{A} it follows immediately:

Property 1: Any point $x \in \mathcal{A}$ has at least one rank-one preimage belonging to \mathcal{A} .

Moreover, we can also state

Property 2: Any point $x \in \mathcal{U}(\mathcal{A}) \setminus \mathcal{A}$ has all its preimages (of any rank) outside \mathcal{A} .

This property holds because otherwise a point in \mathcal{A} would have an image outside \mathcal{A} , and this contradicts the invariance of \mathcal{A} .

Let C be the set of critical points of the map f and C_{-1} be the set of rank-one preimages of the critical points which belong to \mathcal{A} . It is easy to show that it holds

Property 3: *The set C_{-1} is necessarily non-empty: iff f is continuous, \mathcal{A} contains at least one point of local extremum off, while iff f is discontinuous, \mathcal{A} may contain points of discontinuity off, in particular, iff f is a piecewise monotone discontinuous map, \mathcal{A} necessarily includes at least one discontinuity point.*

Clearly, the invariance of \mathcal{A} implies that for every point of \mathcal{A} belonging to C_{-1} all its images of any rank belong to \mathcal{A} . Moreover, it holds the following

Property 4: *The only points interior to \mathcal{A} which can be mapped on the boundary of \mathcal{A} belong to the set C_{-1} .*

To show this consider a point x interior to \mathcal{A} and not belonging to C_{-1} . Then there exists a neighbourhood $\mathcal{U}(x)$ of x (internal to \mathcal{A}) not intersecting C_{-1} so that f is continuous and monotone in $\mathcal{U}(x)$. Then the image $f(\mathcal{U}(x))$ is also internal to \mathcal{A} , which means that x cannot be mapped on the boundary of \mathcal{A} .

Now we can prove Proposition 1. Let us consider a point x at the boundary of \mathcal{A} . Due to the invariance of \mathcal{A} , at least one preimage of x belongs to \mathcal{A} . If x does not belong to C , then its rank-one preimages are either external to \mathcal{A} or belong to the boundary of \mathcal{A} (since, by Property 4, they cannot be internal to \mathcal{A}). Continuing to take the preimages (as at least one preimage on the boundary of \mathcal{A} exists), we can apply the same reasoning for each of them. However, the boundary of \mathcal{A} consists of $2n$ points only, and when no cycle belongs to the boundary a point of C must be reached in a finite number of iterations, while when a cycle belongs to the boundary a preimage of this cycle must be internal to \mathcal{A} and thus it belongs to C_{-1} , so that the cycle consists of critical points.

7.2. Robust chaotic attractors and their bifurcations

An important characteristic of piecewise smooth maps is related to the phenomenon known as *robust chaos* (see [13]). Recall that in smooth maps chaotic attractors are in general not persistent under parameter perturbations. For piecewise smooth maps essentially different bifurcation structures are often observed, in which not only attracting cycles, but also chaotic attractors are robust:

Definition 17: An n -band, $n \geq 1$, chaotic attractor of a map f is **robust** if it persists for parameter values of f belonging to an open region in the parameter space.

This means that neither the chaotic nature of the attractor nor the number of its bands is affected by a small perturbation of parameters.⁷

To give examples of robust chaotic attractors and their bifurcations let us consider the well-known sequence of bifurcations occurring in the skew tent map (4) for decreasing value of the parameter a_R as shown in Figure 17. In this sequence, at the bifurcation point denoted ξ_{RL^2} a pair of 3-cycles, namely, the attracting cycle \mathcal{O}_{RL^2} and repelling cycle \mathcal{O}_{RLR} , emerge due to a *fold BCB*. At the bifurcation point denoted ϑ_{RL^2} the cycle \mathcal{O}_{RL^2} undergoes a degenerate flip bifurcation (DFB, see [76]), and the robust 6-band chaotic attractor appears. For further decreasing value of a_R the bands of this attractor grow and at the point denoted γ_{RL^2} they merge pairwise colliding in the meantime with the repelling cycle \mathcal{O}_{RL^2} . More precisely, it occurs the *first homoclinic bifurcation* of the cycle \mathcal{O}_{RL^2} which has a negative eigenvalue and is located at the boundary of the immediate basin of the 6-band chaotic attractor. Thus, this homoclinic bifurcation causes a so-called *merging bifurcation* which leads from the 6- to a 3-band chaotic attractor.

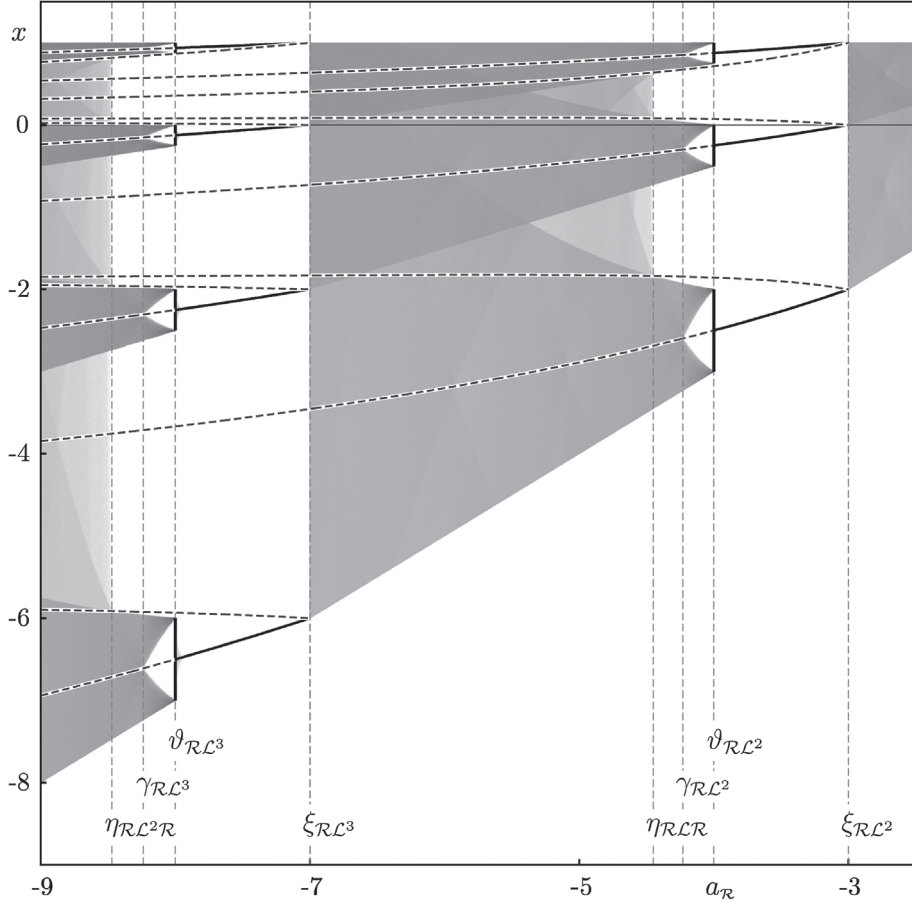


Figure 17. Robust chaotic attractors in the skew tent map (4). Attracting and repelling cycles are shown as solid and dashed curves, respectively. Parameters: $a_L = 0.5$, $\mu = 1$.

Given that the boundaries of the 6-band chaotic attractor are known, namely, the points $c = f(0) = \mu$ and $c_i = f^i(c)$ for $i = 1, \dots, 11$, to obtain the condition of the merging bifurcation one can solve, for example, the equation $c_6 = x_0^{RL^2}$, where $x = x_0^{RL^2} > 0$ is the proper point of the cycle \mathcal{O}_{RL^2} . In such a way we obtain the parameter condition related to the merging bifurcation leading from 6- to 3-band chaotic attractor:

$$\gamma_{RL^2} = \{a_L^4 a_R^3 - a_R + a_L = 0\} \quad (15)$$

The 3-band chaotic attractor exists until the next bifurcation point denoted η_{RLR} in Figure 17, at which it collides with the repelling cycle \mathcal{O}_{RLR} . More precisely, the first homoclinic bifurcation of the cycle \mathcal{O}_{RLR} occurs, which has positive eigenvalue and is located at the immediate basin boundary of the 3-band chaotic attractor. So, this homoclinic bifurcation causes a so-called *expansion bifurcation* leading to the one-band chaotic attractor. The expansion bifurcation is characterized by a sharp increase in size of the attractor.

Given that the boundaries of the 3-bands chaotic attractor are known, which are the critical point c and its images $c_i = f^i(c)$ for $i = 1, \dots, 5$, to obtain the condition of the expansion bifurcation leading to the one-band chaotic attractor one can solve, for example, the equation $c_3 = x_0^{RLR}$, where $x = x_0^{RLR}$ is the proper point of the cycle \mathcal{O}_{RLR} . Proceeding in this way we obtain the condition of this expansion bifurcation:

$$\eta_{RLR} = \{a_L^2 a_R^2 + a_R - a_L = 0\} \quad (16)$$

The one-band chaotic attractor persists until the bifurcation point ξ_{RL^3} at which the next pair of cycles appear via a fold BCB, namely the attracting and repelling 4-cycles \mathcal{O}_{RL^3} and \mathcal{O}_{RL^2R} , respectively. These cycles undergo a similar sequence of bifurcations.

Recall that a *final bifurcation* of a chaotic attractor is also caused by a homoclinic bifurcation of a repelling cycle located on the immediate basin boundary of the attractor. However, it results in the transformation of this attractor in a chaotic repellor. For the skew tent map the final bifurcation, occurring at

$$\chi_L = \{a_R(1 - a_L) - a_L = 0\} \quad (17)$$

is caused by the first homoclinic bifurcation of the fixed point \mathcal{O}_L (when the critical point $c = \mu$ satisfies $f(c) = \mathcal{O}_L$), after which the interval $J = [f(c), c]$ is no longer absorbing, and almost all the trajectories, except the chaotic repellor, diverge.

Note that conditions for the merging and expansion bifurcations in the skew tent map can be obtained in a more elegant way (see, e.g. [75] for a survey).

Two examples of expansion bifurcation in the discontinuous map (2) can be seen in Figure 16, related to the transitions between three- and one-band chaotic attractors. They are caused by the homoclinic bifurcation of the 2-cycle \mathcal{O}_{LR} . This cycle is not homoclinic for the parameter values related to the three-band attractor and it is double-side homoclinic after the expansion bifurcation. The parameter values related to one expansion bifurcation can be found by solving the equation $x_0^{LR} = c_1^r$, or $x_1^{LR} = c_2^r$, while the parameter values related to the other expansion bifurcation by solving any of the equations $x_0^{LR} = c_1^\ell$, or $x_1^{LR} = c_2^\ell$. In any way we obtain, respectively, the following two conditions of the expansion bifurcations:

$$\eta_{LR}^r = \left\{ \frac{\mu_L}{\mu_R} = \frac{1 + a_R a_L^2 - a_L}{1 - a_R a_L - a_R} \right\} \quad \text{and} \quad \eta_{LR}^\ell = \left\{ \frac{\mu_L}{\mu_R} = \frac{1 - a_R a_L - a_L}{1 + a_R^2 a_L - a_R} \right\}$$

7.3. Cyclicity of chaotic attractors

The cyclicity of multi-band chaotic attractors often appears to be a useful property. It allows, for example, to reduce a problem related to an m -band attractor of a map f to one related to a one-band attractor of the m th iterate f^m . However, the question arises in which cases multi-band chaotic attractors are cyclic (often denoted then as *cyclic chaotic intervals*), and in which not (see [11]).

Let a chaotic attractor \mathcal{A} of a map $x_{n+1} = f(x_n)$ consist of $m > 1$ disjoint bands (intervals) \mathcal{B}_i , $i = 0, \dots, m - 1$, then \mathcal{A} is *cyclic* if

$$f(\mathcal{B}_i) = \mathcal{B}_{i+1}, \quad i = 0, \dots, m - 2 : \quad f(\mathcal{B}_{m-1}) = \mathcal{B}_0, \quad (18)$$

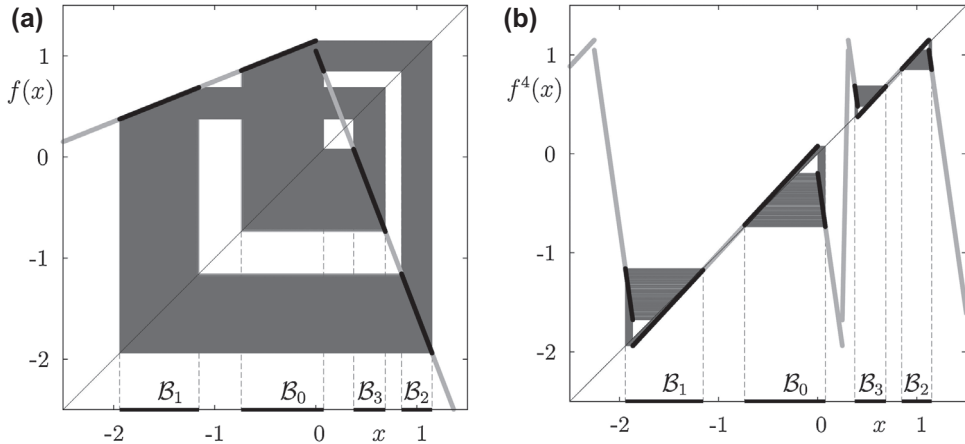


Figure 18. In (a): Cyclic 4-band chaotic attractor of map (2) at $a_L = 0.4$, $a_R = -2.6$ $\mu_L = 1.15$ $\mu_R = 1.05$; In (b): four coexisting one-band attractors of the fourth iterate f^4 .

It can be shown (see e.g. [3,23,62]) that the following property holds:

Property 5: *Multi-band chaotic attractors in continuous maps are always cyclic, while in discontinuous maps they may be cyclic or not.*

For example, any m -band chaotic attractor, $m \geq 2$, of the skew tent map (4) (see Figure 17) is cyclic.

The 4-band chaotic attractor of discontinuous map (2) shown in Figure 18(a) is also cyclic, and as a result, map f^4 has four one-band chaotic attractors (see Figure 18(b)). In fact, in the considered case the jump of the system function at the discontinuity point $\Delta = |\mu_L - \mu_R|$ is small compared with the size of the bands of the attractor. Given that at $\Delta = 0$ the system function is continuous and therefore the attractor is cyclic, it is not surprising that for small enough values of Δ this property persists.

As a next example let us consider the 3-band chaotic attractor of map (2) shown in Figure 19(a). In this case we have $f(\mathcal{B}_1) = \mathcal{B}_2$ and $f(\mathcal{B}_2) = \mathcal{B}_0$ but for the band \mathcal{B}_0 it can clearly be seen that $f(\mathcal{B}_0) \subsetneq \mathcal{B}_0 \cup \mathcal{B}_1$. As a consequence, the attractor is not cyclic, since the band \mathcal{B}_0 is mapped not only onto \mathcal{B}_1 but partially into itself. If one considers the third iterate f^3 , it also has a 3-band chaotic attractor (see Figure 19(b)), as each band is not invariant by f^3 .

Note also that not every acyclic m -band chaotic attractor corresponds to a single m -band chaotic attractor of the m th iterate. As an example Figure 20(a) shows a 4-band chaotic attractor of map (2), such that the fourth iterate of map (2) has two coexisting 2-band attractors, as shown in Figure 20(b).

In all the considered examples the bands of acyclic attractors of map (2) behave differently depending on whether they contain the point of discontinuity (border point) $x = 0$ or not. In fact, the bands not containing the border point (\mathcal{B}_1 and \mathcal{B}_2 in the example shown in Figure 19, as well as $\mathcal{B}_1, \mathcal{B}_2$ and \mathcal{B}_3 in Figure 20) have one successor band. By contrast, the band containing the border point (\mathcal{B}_0 in both examples) has more than one successor band and this breaks the cyclicity. Using Property 3 we can introduce a criterion which allows us to distinguish between cyclic and acyclic attractors of a piecewise monotone discontinuous map with one border point:

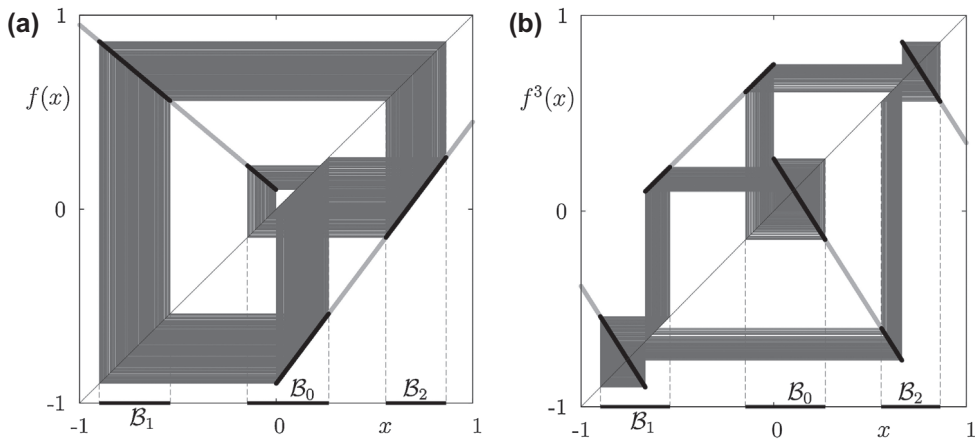


Figure 19. In (a): An acyclic 3-band chaotic attractor of map (2) at $a_L = -0.85$, $a_R = 1.35$ $\mu_L = 0.1$ $\mu_R = -0.9$; In (b): The corresponding acyclic 3-band chaotic attractor of the third iterate f^3 .

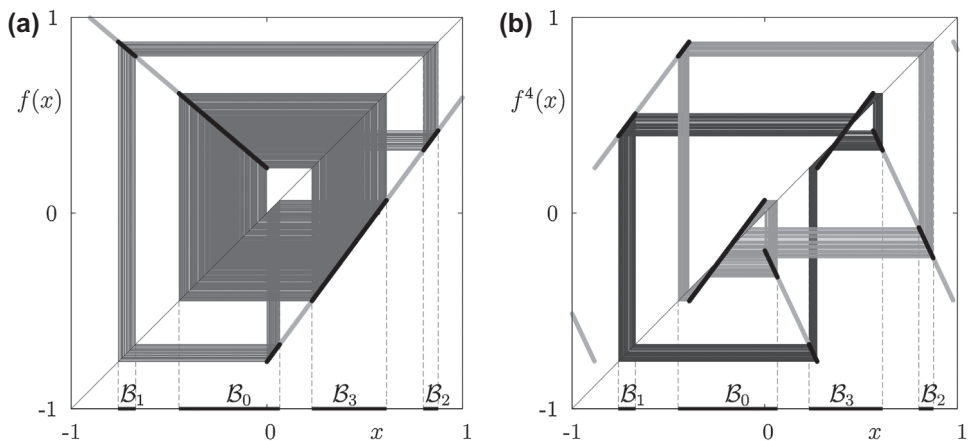


Figure 20. In (a): An acyclic 4-band chaotic attractor of map (2) at $a_L = -0.85$, $a_R = 1.35$ $\mu_L = 0.23$ $\mu_R = -0.76$; In (b) Two coexisting 2-band attractors of the fourth iterate f^4 .

Property 6: A multi-band chaotic attractor is cyclic if the band containing the border point is mapped in only one band, and acyclic otherwise.

8. Coexistence of attractors

Let us now discuss which attractors can coexist in a piecewise smooth 1D map f . First recall that the border points of the n th iterate f^n are given by the border points of f and their preimages. The same applies also to the points of smooth extrema of f^n . These points confine the intervals on which f^n is given by different compositions of the monotone branches of f , that is, the intervals of monotonicity of f^n (which may be bounded on both sides or one-side unbounded). If the map f is piecewise monotone, then each branch of f^n is monotone as well. Similarly, if the map f is piecewise linear, then the map f^n consists of linear branches. This simple observation helps us to prove the following:

Proposition 2: *Any attracting cycle of a piecewise linear map attracts at least one border point.*

As we consider an attracting n -cycle for some $n \geq 1$, the iterate f^n must have n attracting fixed points associated with the corresponding linear branches. If the cycle is globally attracting, this proposition is obviously true. Otherwise, function f^n must be a linear contraction in each interval bounded by at least one border point \tilde{x} (which is a preimage of a border point of f). Then the image of the point \tilde{x} by f^n converges to the corresponding fixed point. Therefore, at least one border point of f converges to the n -cycle.

As any chaotic attractor of a piecewise monotone map defined on two partitions includes the border point of the map, it follows that

Proposition 3: *Two chaotic attractors cannot coexist in a piecewise monotone map with one border point (continuous or discontinuous).*

Furthermore, it holds

Proposition 4: *In a piecewise linear 1D map with one border point, a chaotic attractor cannot coexist with any other attractor.*

As the border point belongs to the chaotic attractor and hence both the left and the right limit values of the function at the border point also belong to the chaotic attractor. Therefore, no other attractor is possible (neither a chaotic attractor nor a cycle) as no other border point exists.

Propositions 4 and 2 immediately imply the following well-known result:

Proposition 5: *A continuous piecewise linear 1D map with one kink point can have at most one attractor.*

Indeed, if the attractor is chaotic, it is the unique attractor, as stated in Proposition 4. Otherwise, if the attractor is a cycle, the property given in Proposition 2 implies that it is unique as well, because the map has only one kink point at which it is continuous.

For discontinuous maps the situation is different. In this case, the coexistence of attractors is possible, but only for cycles:

Proposition 6: *A discontinuous piecewise linear 1D map with one border point can have at most two attractors. If two attractors coexist, both of them are cycles.*

As we have already mentioned, if the attractor is chaotic it cannot coexist with any other attractor. If the attractor is a Cantor set attractor or an interval filled with quasiperiodic trajectories, it is globally attracting and hence unique. So, the only remaining possibility are cycles. As by assumption the map has two critical points, at most two attracting cycles can coexist.

The coexistence of two cycles in map (2) is illustrated in Figure 21(a). In this example the critical point c^l belongs to the basin of the 2-cycle, while the critical point c^r belongs to the basin of the 4-cycle. The basins are separated from each other by the border point and its preimages, which are accumulating (inside the absorbing interval) to the repelling fixed point in the right partition, and related preimage in the left partition.

It is worth noting that the properties of the piecewise linear 1D maps with one border point stated above cannot be generalized for piecewise monotone 1D maps. In fact, for these maps the basins of coexisting attractors may be separated from each other not only by the preimages of the critical points but also by repelling cycles. For example, the map shown in Figure 21(b) is continuous and piecewise linear, and hence its 4-band chaotic

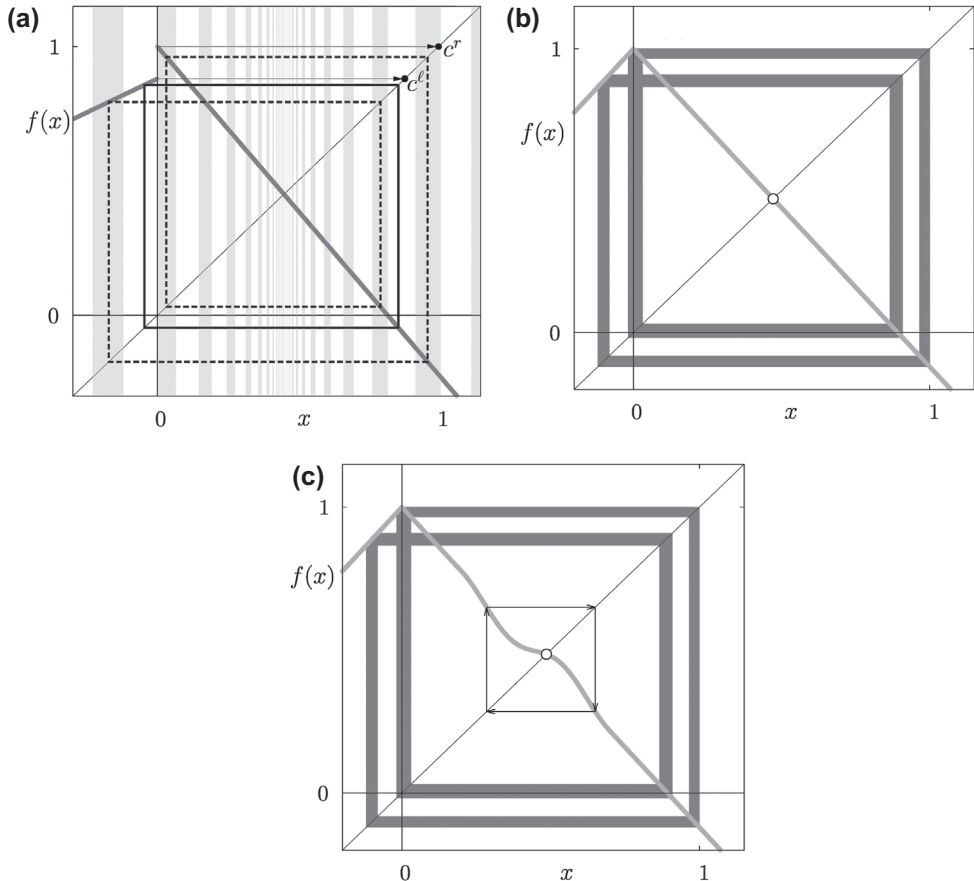


Figure 21. In (a): Coexisting attracting 2- and 4-cycles of map (2) shown with solid and dashed lines, respectively; The basin of the 4- and 2-cycles are shown in grey and white, respectively; The critical points c^l and c^r are marked; Parameters: $a_L = 0.5$, $a_R = -1.22$, $\mu_L = 0.88$, $\mu_R = 1$. In (b): Unique 4-band chaotic attractor of a continuous piecewise linear map. In (c): Coexisting 4-band chaotic attractor and an attracting fixed point in a piecewise smooth continuous map. Additionally, the repelling 2-cycle is shown, which bounds the immediate basin of the fixed point.

attractor is unique. In Figure 21(c) the map is modified in such a way that the fixed point in the right partition is attracting. This modification of the map also causes a repelling 2-cycle to appear, and this 2-cycle forms the boundary of the immediate basin of the attracting fixed point.

As one more example let us consider the linear-logistic map defined by:

$$x_{n+1} = \begin{cases} f_L(x_n) = rx_n & \text{if } x_n \leq \bar{x} \\ f_R(x_n) = ax_n(1-x_n) & \text{if } x_n \geq \bar{x} \end{cases} \quad \text{with } \bar{x} = 1 - \frac{r}{a} \quad (19)$$

(see [73,74]). It can easily be shown that for $a < 2r$ the image of the border point \bar{x} is not a critical point and there exists a ‘smooth’ critical point $c = \frac{a}{4}$. The coexistence of two cycles in map (19) is illustrated in Figure 22, where an attracting 2-cycle and an attracting 4-cycle coexist, and their immediate basins are separated by a repelling 4-cycle (born at a

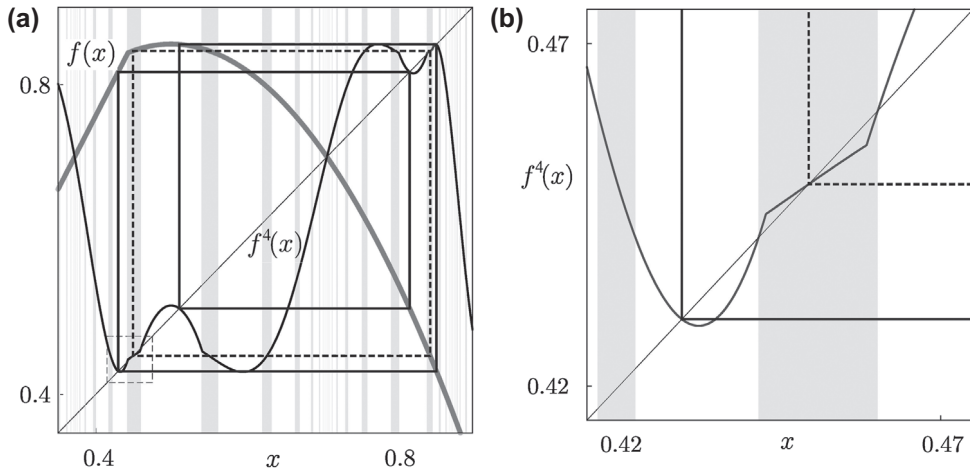


Figure 22. In (a): Coexisting attracting 2- and 4-cycles of map (19) are shown with dashed and solid lines, respectively; Parameters: $a = 3.41$, $r = 1.9$. The basins of the 2- and 4-cycles are shown in grey and white, respectively. In (b) the window indicated in (a) is enlarged, which shows a portion of f^4 .

fold bifurcation together with the attracting 4-cycle) and its rank-one preimage. Hereby, one of the cycles attracts the smooth critical point and the other one the kink point.

9. First return map

The *first return map* which often appears to be very useful for investigation of the dynamics of a map, is defined as follows:

Definition 18: For a map $f : I \rightarrow I$ the **first return map** $g : J \rightarrow J$, $J \subset I$, associates each point $x \in J$ with its image $f^{k_x}(x)$ such that $f^{k_x}(x) \in J$ and $f^i(x) \notin J$ for $1 \leq i \leq k_x - 1$.

There is a correspondence between the dynamics of map g and the dynamics of map f . If each point $x \in I \setminus J$ is mapped in a finite number of iterations in J , then this correspondence is one-to-one.

The simplest example of a first return map g for a map f which has an attracting n -cycle is the map g defined on a proper neighbourhood J of any point of the cycle by the n th iterate f^n . An advantage to consider g instead of f in this case is obvious: One can deal with a fixed point of g instead of an n -cycle of f .

When dealing with a piecewise smooth map with one border point, an interval J around the border point is often considered. In particular, for map (2) it is often useful to consider the first return map defined in an interval J which includes the border point $x = 0$.

As an example let us consider map (2) in the increasing / increasing configuration as shown in Figure 23(a). At the considered parameter values the only invariant set of the map inside the absorbing interval $I = [-1, 1]$ is the attracting 22-cycle $\mathcal{O}_{RL(RLRL)^4}$. The first return map g for map (2) defined on the interval

$$J = [f_R \circ f_L \circ f_R(0), f_R \circ f_L(0)] \quad (20)$$

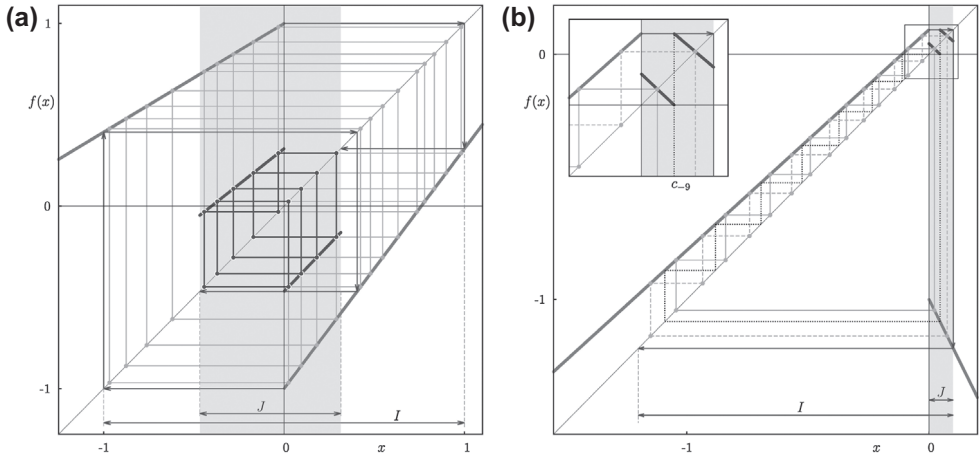


Figure 23. In (a): First return map (shown with black lines) for map (2) on the interval J (marked grey) given by Equation (20). The attracting 22-cycle of map (2) corresponds to the 9-cycle $\mathcal{O}_{L(LR)^4}$ of the first return map. Parameters: $a_L = 0.59523$, $a_R = 1.31453$, $\mu_L = 1$, $\mu_R = -1$. In (b): First return map for map (2) on the interval J given by Equation (22). Two coexisting attracting cycles \mathcal{O}_{RL^7} and \mathcal{O}_{RL^8} are shown with solid and dashed grey lines, respectively. Dashed black lines indicate preimages of $x = 0$. The inset shows the marked rectangle enlarged. Parameters: $a_L = 0.9$, $a_R = -2$, $\mu_L = 0.1$, $\mu_R = -1$.

is given by two linear branches, $f_R \circ f_L(x)$ and $f_R \circ f_L \circ f_R(x)$, and has the same point of discontinuity $x = 0$ as the original map:

$$x_{n+1} = g(x_n) = \begin{cases} g_L(x_n) = f_R \circ f_L(x_n) & \text{if } x_n < 0 \\ g_R(x_n) = f_R \circ f_L \circ f_R(x_n) & \text{if } x_n > 0 \end{cases} \quad (21)$$

It can easily be seen in Figure 23(a) that the interval J represents the absorbing interval for g and the only invariant set of this map is the attracting 9-cycle $\mathcal{O}_{L(LR)^4}$. The correspondence between the 22-cycle of the original map and the 9-cycle of the first return map is also obvious: The points of the 22-cycle of the original map located inside the interval J represent the points of the 9-cycle of the first return map, moreover, the symbolic sequence of the 22-cycle is obtained substituting in the symbolic sequence of the 9-cycle the symbol L with RL and the symbol R with RLR .

In some cases it is preferable to define the first return map on an interval which does not contain the border point of the original map. In such cases, when the original map is piecewise smooth, the border points of the first return map are given by some preimages of the border points of the original map. As an example, Figure 23(b) shows the first return map for map (2) defined on the interval

$$J = [0, f_L(0)] \quad (22)$$

At the considered parameter values the map is in the increasing / decreasing configuration, it has coexisting attracting cycles \mathcal{O}_{RL^7} and \mathcal{O}_{RL^8} . The first return map consists of linear branches $f_L^7 \circ f_R(x)$, $f_L^8 \circ f_R(x)$ and its discontinuity point is the first preimage of $x = 0$

located inside J , namely $c_{-9} = f_R^{-1} \circ f_L^{-7}(0)$:

$$x_{n+1} = g(x_n) = \begin{cases} g_L(x_n) = f_L^7 \circ f_R(x_n) & \text{if } x_n < c_{-9} \\ g_R(x_n) = f_L^8 \circ f_R(x_n) & \text{if } x_n > c_{-9} \end{cases} \quad (23)$$

As one can see in Figure 23(b), the points of the cycles located inside the interval J represent the fixed points of the first return map.

10. Piecewise increasing maps

Let us consider now the family of piecewise smooth maps $f : I \rightarrow I$, $I \subset \mathbb{R}$, defined as follows:

$$x_{n+1} = f(x_n) = \begin{cases} f_L(x_n) & \text{if } x_n < 0 \\ f_R(x_n) & \text{if } x_n > 0 \end{cases} \quad (24)$$

with $I = [f_R(0), f_L(0)]$ and satisfying the following properties:

- the functions f_L, f_R are continuous and strictly increasing on $[f_R(0), 0]$ and $[0, f_L(0)]$, respectively;
- the map does not have fixed points in the interval $(f_R(0), f_L(0))$.

An interest towards map (24), which has been studied by many researchers, is explained by the fact that it is associated with the Poincaré return map of Lorenz-like flows. Due to this property map (24) is frequently referred to as *Lorenz map*.⁸ Note that BCBs in Lorenz maps correspond to homoclinic bifurcations in the associated flows. For more details see, e.g. [17, 24, 31, 32, 37–40, 43, 44, 52, 70, 77].

To study the dynamics of Lorenz maps the return map (not necessarily the first) in a neighbourhood of the discontinuity point $x = 0$ is often used, also referred to as *renormalization*. It is worth to note also that it may happen that although one or both of the functions f_L and f_R are decreasing, an appropriate return map can be constructed in such a way that it has two increasing branches, and therefore the results discussed below are applicable for such maps as well.

10.1. Invertibility on the absorbing interval

The key point in the description of the dynamics of a Lorenz map regards the invertibility of the map on the interval I . According to that, we distinguish between the following three cases:

- (1) *Gap maps*: If

$$f_R \circ f_L(0) < f_L \circ f_R(0), \quad (25)$$

then each point $x \in I$ has either a unique preimage or no preimages inside I . The nonempty interval $Z_0 \subset I$, the points of which have no preimages in I , is called a *gap*: $Z_0 = (f_R \circ f_L(0), f_L \circ f_R(0))$ (see Figure 24(a)). The maps which satisfy the condition (25) are called *gap maps* [17]. This case is also referred to as *nonoverlapping case* [49].

- (2) *Circle homeomorphisms*: If

$$f_R \circ f_L(0) = f_L \circ f_R(0), \quad (26)$$

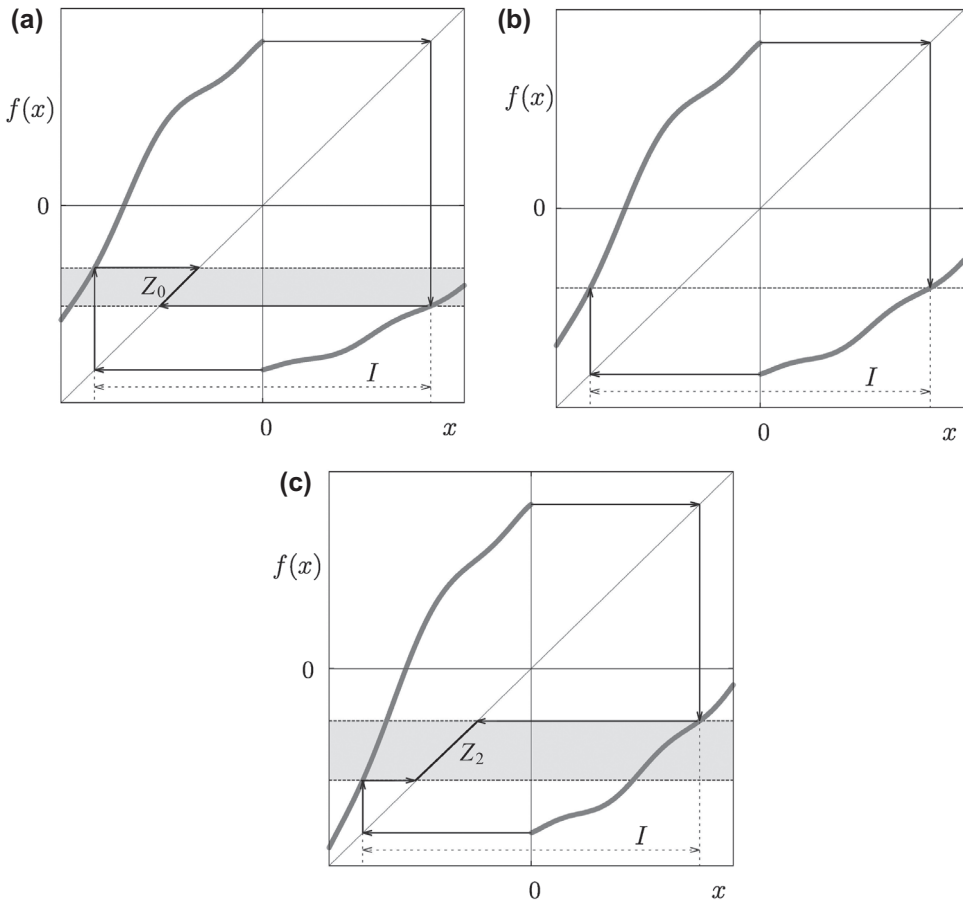


Figure 24. Three characteristic cases of piecewise increasing maps: (a) a gap map where the gap Z_0 is shown grey, (b) a circle homeomorphism, (c) an overlapping map where the overlapping interval Z_2 is shown grey.

(see Figure 24(b)), then each point $x \in I$ has a unique preimage in I , except for the point $p = f_R \circ f_L(0) = f_L \circ f_R(0)$, which has two distinct rank-one preimages, but only one preimage of rank two, namely $x = 0$. In this case the map can be identified with a circle homeomorphism studied extensively since the works by Poincaré and Denjoy [26,69]. For this reason map (24) satisfying condition (26) is called *circle homeomorphism*.

(3) *Overlapping maps:* If

$$f_R \circ f_L(0) > f_L \circ f_R(0), \quad (27)$$

then each point $x \in I$ has either a unique preimage or two preimages inside I . The nonempty interval $Z_2 \subset I$ in which the points have two preimages in I is given by $Z_2 = [f_L \circ f_R(0), f_R \circ f_L(0)]$ (see Figure 24(c)). This case is also called *overlapping case* [17,49].

To describe the dynamics of a Lorenz map, which differs significantly in the three cases listed above, the concept of a *rotation number* appears to be very useful. For a piecewise

smooth map f defined on two partitions $x < 0$ and $x > 0$, it is defined as follows (see, e.g. [49]):

Definition 19: The **rotation number** $\rho(x)$ for a point x is defined by

$$\rho(x) = \lim_{n \rightarrow \infty} \frac{1}{n} \sum_{k=0}^n \chi_r(f^k(x)) \quad (28)$$

where χ_r is the characteristic function of the right partition:

$$\chi_r(x) = \begin{cases} 0 & \text{if } x < 0 \\ 1 & \text{otherwise} \end{cases} \quad (29)$$

10.2. Gap maps

Recall first an important property of the gap maps related to their rotation numbers:

Property 7: If map (24) is a gap map then all the points $x \in I$ have the same the rotation number $\rho(x) = \rho$.

For the proof see, for example, [49,63]. Due to this property, in the case of a gap map we can consider the rotation number ρ of the map and not only of particular points.

It can easily be shown that neither the gap Z_0 nor any of its images can contain any point of some invariant set. Let us define the sets A and B as

$$B = \bigcup_{n=0}^{\infty} f^n(Z_0), \quad (30)$$

$$A = I \setminus B. \quad (31)$$

Then the following holds:

Proposition 7: If map (24) is a gap map, then every invariant set of the map in I belongs to the set A .

Otherwise a point of the invariant set would have a preimage in Z_0 , which is a contradiction.

The invariance of set A can be shown by excluding the other possibilities. Firstly, we can exclude the case $A \subsetneq f(A)$, since that would mean that there exists a point $p \in A$ with $f(p) \notin A$, that means $f(p) \in B$. This is clearly not possible, since for each point in B its preimage in I (if one exists) belongs to B as well. Then we can also exclude $f(A) \subsetneq A$. Indeed, in this case a point $p \in A \setminus f(A)$ must exist, for which no preimage p_{-1} exists in A (as otherwise $p \in f(A)$). This implies that either p has no preimages, which is not possible as in this case we have $p \in Z_0 \subset B$, or p_{-1} and thus p belongs to B , which is also not possible.

It is worth to note that set A , being invariant and containing all invariant sets of map (24), may but does not need to be an attractor. As we shown below, A is an attractor if the rotation number of the map is irrational, while for a rational rotation number A is an attracting set which may be an attractor or not.

Proposition 8: If map (24) is a gap map and its rotation number ρ is rational, then the ω -limit set $\omega(x)$ for all $x \in I$ is a cycle. The map may have several cycles, but all of them have the same period. The rotation number persists under parameter perturbation.

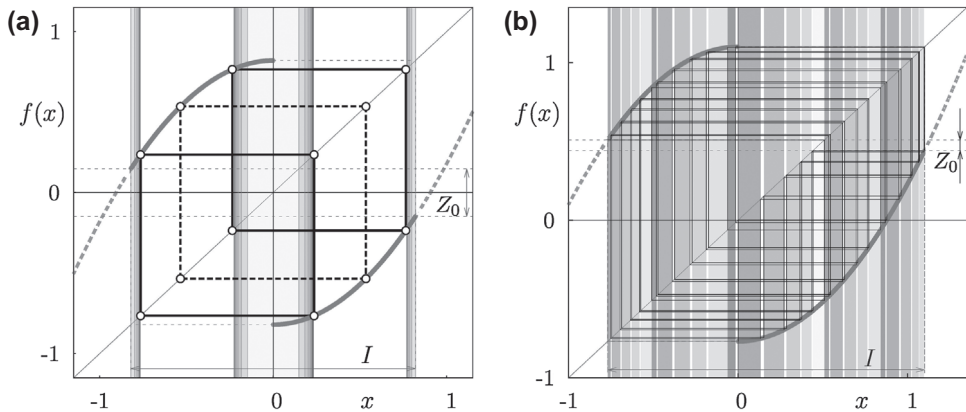


Figure 25. Invariant sets of map (32) in the case that it is a gap map. The lightest grey region indicates Z_0 and the regions of increasing darkness correspond to images of Z_0 of increasing rank. In (a): Two attracting (shown with solid lines) and one repelling (shown with dashed lines) 2-cycles in the case of rotation number $\rho = \frac{1}{2}$. In (b): A Cantor set attractor in the case of the irrational rotation number $\rho = \frac{1}{\sqrt{5}}$. Parameter values (corresponding to the points marked with (a) and (b) in Figure 26): $\mu_L = 0.82$, $\mu_R = -0.82$ (a); $\mu_L = 0.88$, $\mu_R \approx -0.7102239164561458$ (b).

In the case of a piecewise linear gap map (2) with a rational rotation number the cycle is necessarily unique and attracting (in this case set A is an attractor) [43,52]. In general, several attracting and repelling cycles may exist (see Figure 25(a)). Moreover, the interval I may contain sub-intervals filled with neutral cycles.

Considering the preimages of the discontinuity point $x = 0$ and its α -limit set $\alpha(0)$, the results proved in [79] imply the following

Proposition 9: *If map (24) is a gap map then*

- (1) *if the discontinuity point $x = 0$ belongs to the interval Z_0 , then the rotation number of the map is $\rho = \frac{1}{2}$;*
- (2) *if a preimage of finite rank of the discontinuity point $x = 0$ belongs to the interval Z_0 , then the rotation number of the map is rational;*
- (3) *if $\alpha(0)$ is a finite set then the rotation number of the map is rational;*
- (4) *if $\alpha(0)$ is an uncountable set then the rotation number of the map is irrational.*

From Property 7 it follows that if the map has an irrational rotation number, no cycle can exist (as a cycle must have a rational rotation number).

Proposition 10: *If map (24) is a gap map and its rotation number ρ is irrational, then the ω -limit set $\omega(x)$ for all $x \in I$ is a Cantor set attractor. This Cantor set attractor is unique.*

To explain this Proposition let us recall the concept of a *wandering interval*.

Definition 20: An interval J is called a **wandering interval** for a map f if

- (a) the images $f^n(J)$ of J are disjoint for all $n > 0$;
- (b) the ω -limit set of J is not a single cycle.

It turns out that the following Proposition holds:

Proposition 11: *If map (24) is a gap map and its rotation number ρ is irrational, then the gap Z_0 is a wandering interval.*

The property (b) in the definition of a wandering interval is clearly satisfied for a gap map with an irrational rotation number, as in this case a cycle cannot exist. Property (a) is also satisfied: if we assume the contrary, then two images of the gap, say $f^n(Z_0)$ and $f^m(Z_0)$ with $n \neq m$, overlap and there exists a point $p \in f^n(Z_0) \cap f^m(Z_0)$. Thus points r and s must exist in Z_0 such that $f^n(r) = f^m(s) = p$, that is, assuming $n < m$, $r = f^{n-m}(s)$, which is not possible. Hence, for all $n \neq m$ the images of the gap $f^n(Z_0)$ and $f^m(Z_0)$ are disjoint.

As a consequence, a Cantor set attractor of a gap map (24) with an irrational rotation number is given by the set A (see an example in Figure 25(b)). Clearly, as this set is uniquely defined, the Cantor set attractor is a global attractor. In this case the ω -limit set for each point $x \in I$ is the Cantor set attractor.

As shown in [49], the behaviour of gap maps under variation of parameters is described by the following

Proposition 12: *For a family of gap maps depending smoothly on some parameter ξ , the rotation number ρ is a function $\rho(\xi)$ which takes rational values on nonempty intervals and irrational values on a Cantor set of values of zero Lebesgue measure.*

In the case of a piecewise linear gap map (2) the corresponding bifurcation structure in a parameter space is formed by BCB boundaries of regions related to attracting cycles, and is referred to as *period adding structure*. In general the bifurcation structure may be more complicated, as the cycles may appear and disappear not only via BCBs but also via smooth fold bifurcations.

To illustrate the properties of gap maps let us consider the following piecewise quadratic map:

$$x_{n+1} = f(x_n) = \begin{cases} f_L(x_n) = -x_n^2 + \mu_L & \text{if } x_n < 0 \\ f_R(x_n) = x_n^2 + \mu_R & \text{if } x_n > 0 \end{cases} \quad (32)$$

which represents one of the standard models of the Poincaré return maps of the Lorenz-like flows in the so-called orientable case under the assumption that the saddle-index of the origin is larger than one. For the details on this map and its bifurcation structure shown in Figure 26 we refer to [33] and references therein.

Condition (25) holds for map (32) for values of parameters μ_L, μ_R belonging to the following region in the parameter space:

$$\{(\mu_L, \mu_R) \mid \mu_L^2 + \mu_R < -\mu_R^2 + \mu_L\} \quad (33)$$

For such parameter values map (32) is a gap map. In Figure 26 this region is located below the curve marked with C_1 . Accordingly, for parameter values inside this region the attractors of map (32) are either attracting cycles (persistent under parameter perturbations) or Cantor set attractors (not persistent under parameter perturbations). For example, at the parameter values corresponding to the point marked with (a) in Figure 26 the map has rational rotation number $\rho = \frac{1}{2}$. As shown in Figure 25(a), at these parameter values the map has three 2-cycles, two of which are attracting and one is repelling. In this case, the set B defined by Equation (30) is given by three groups of intervals (one of them, located around the point of discontinuity is bounded by two points of different attracting 2-cycles, and the image of this group of intervals is given by two other groups of intervals each of which is bounded by the related critical point and the other point of the attracting 2-cycle). The ω -limit set for all $x \in Z_0$ is given by a 2-cycle. The complementary set A (defined by

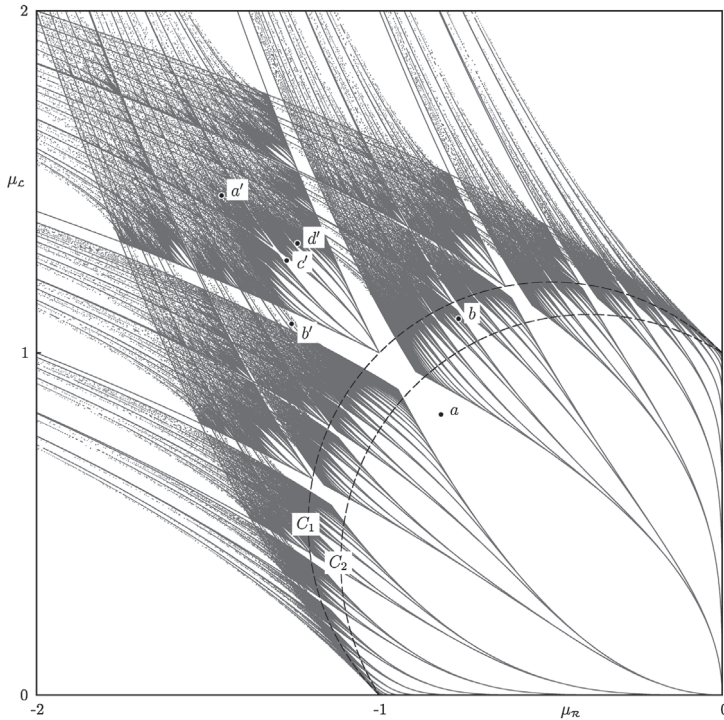


Figure 26. Bifurcation structure of map (32). Inside the region confined by the curve C_1 the map (32) represents a gap map, and outside – an overlapping map. Parameter values marked with (a) and (b) correspond to Figure 25(a) and (b). Parameter values marked with a' – d' correspond to Figure 30(a)–(d). The bifurcation scenarios along the curves marked with C_2 , C_1 are shown in Figures 27 and 28, respectively.

Equation (31)) is given by two intervals inside which the points of the repelling 2-cycle are located.

The situation shown in Figure 25(b) is different. At these parameter values (marked with (b) in Figure 26) the map has irrational rotation number $\rho = \frac{1}{\sqrt{5}}$. As a consequence, the map has a Cantor set attractor given by set A and set B belongs to its total basin of attraction restricted to the interval I .

A typical bifurcation scenario of map (32) under the variation of parameters inside the region where the map represents a gap map is shown in Figure 27. To preserve the symmetry of the structure the parameters are varied along the curve marked with C_2 in Figure 26. As one can see, the rotation numbers form the well-known Devil's staircase structure (see Figure 27(c)) in which rational values correspond to intervals and irrational values to points belonging to a Cantor set (of zero measure). The overall period adding structure is typical for piecewise smooth gap maps. The main difference between the piecewise linear map (2) and the piecewise quadratic map (32) is that in the latter case attracting cycles of the same period may coexist (this is clearly visible in Figure 25 and Figure 27(a) for the 2-cycles). By contrast, in the case of map (2) every attracting cycle is necessarily unique.

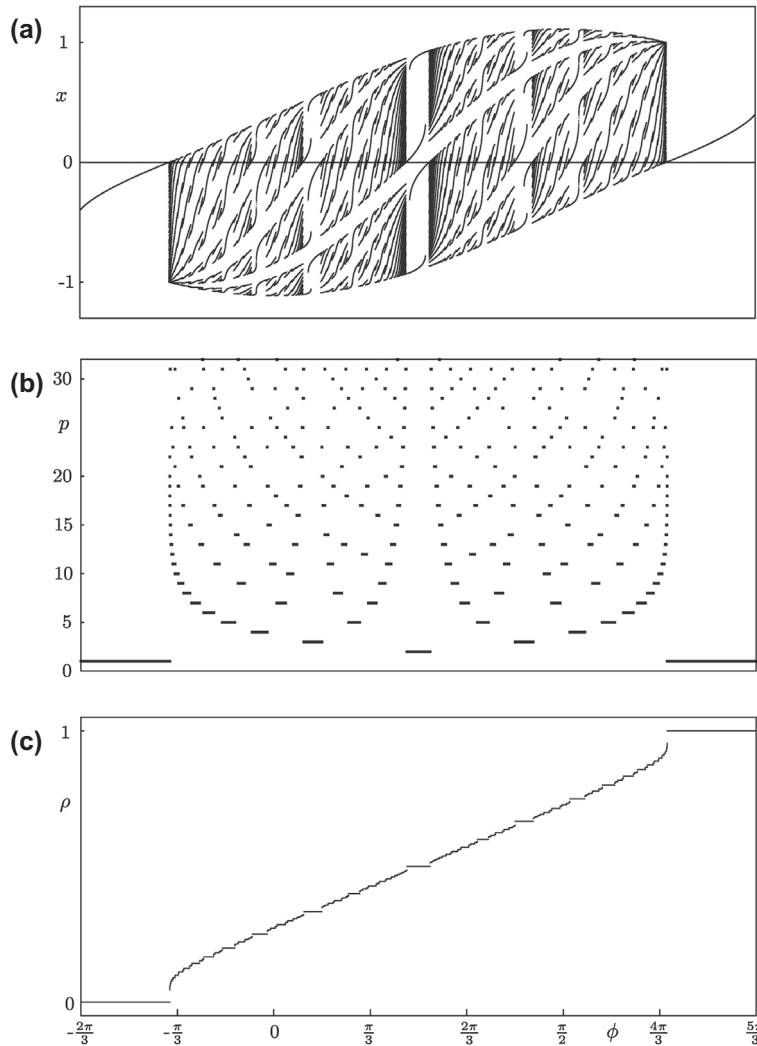


Figure 27. In (a): Bifurcation diagram of map (32) along the curve marked with C_2 in Figure 26; Related diagrams of period p and rotation number ρ are shown in (b) and (c), respectively.

10.3. Circle homeomorphisms

Some of the properties of invertible circle maps are similar to the properties of gap maps. In particular,

Property 8: *If map (24) is a circle homeomorphism then all the points $x \in I$ have the same the rotation number $\rho(x) = \rho$.*

Hence, also in the case of a circle homeomorphisms we can speak about the rotation number ρ of the map and not only of particular points.

The simplest case of a circle homeomorphism is the *rotation map* $R_\rho : [0, 1] \rightarrow [0, 1]$ defined by

$$x_{n+1} = R_\rho(x_n) = \begin{cases} x + \rho & \text{if } 0 \leq x_n < 1 - \rho \\ x + \rho - 1 & \text{if } 1 - \rho < x_n \leq 1 \end{cases} \quad (34)$$

The parameter $\rho \in (0, 1)$ represents the rotation number of the map. The behaviour of map (34) depends on ρ as follows:

Proposition 13: *If the rotation number ρ of map (34) is rational, then the complete interval $I = [0, 1]$ is filled with neutral cycles. If ρ is irrational, the interval I is filled with quasiperiodic orbits, and each of them is dense in I .*

The question arises concerning the extent to which the behaviour of a general circle homeomorphism is similar to the behaviour of map (34). Certainly, we have to distinguish between rational and irrational rotation numbers. The case of a rational rotation number is similar to the one in the gap maps [63]:

Proposition 14: *If map (24) is a circle homeomorphism and its rotation number ρ is rational, then the ω -limit set $\omega(x)$ for all $x \in I$ is a cycle. The map may have several cycles, but all of them must have the same period.*

If a circle homeomorphism is defined by two linear branches, as for example the map (2), it is conjugate to map (34), and thus in case of a rational rotation each point of the interval I is periodic, so that the complete interval I is filled with cycles of the same period. In general, several attracting and repelling cycles may exist, as well as intervals filled with neutral cycles.

Investigation of the circle homeomorphisms with irrational rotation numbers originates from the works by Poincaré who proved that every circle homeomorphism with an irrational rotation number ρ is semi-conjugate to map (34). However, this result does not mean that every circle homeomorphism shows the same behaviour as map (34), since the interval filled with quasiperiodic trajectories may be mapped by semi-conjugacy to a Cantor set attractor. A stronger result was proved by Denjoy [26], according to which if a circle diffeomorphism of class C^2 has an irrational rotation number ρ then it is conjugate to an irrational rotation. Moreover, in a weaker assumption, if a circle diffeomorphism has derivative of bounded variation, then the map is conjugate to map (34). If the derivative of a circle diffeomorphism is of unbounded variation then the map may have a wandering interval and therefore a Cantor set attractor. Moreover, there exists also an approach which makes it possible to construct a circle map with a Cantor set attractor for any given irrational rotation number (see [26,63]). Consequently, it holds

Proposition 15: *If map (24) is a circle homeomorphism with rational rotation number ρ , then either the map has a Cantor set attractor strictly included in I , or the interval I is an attractor densely filled with quasiperiodic orbits (which occurs when the map is conjugate to an irrational rotation).*

Note that properties (3) and (4) in Proposition 9 hold also for a circle homeomorphism.

The behaviour of circle homeomorphisms under variation of parameters is described by the following

Proposition 16: *For a family of circle homeomorphisms depending smoothly on some parameter ξ , the rotation number ρ as a function of ξ represents a function which takes*

- (1) *either rational values on nonempty intervals and irrational values on a Cantor set of parameter values;*
- (2) *or rational values on a countable set of parameter values and irrational values on an uncountable set of positive measure.*

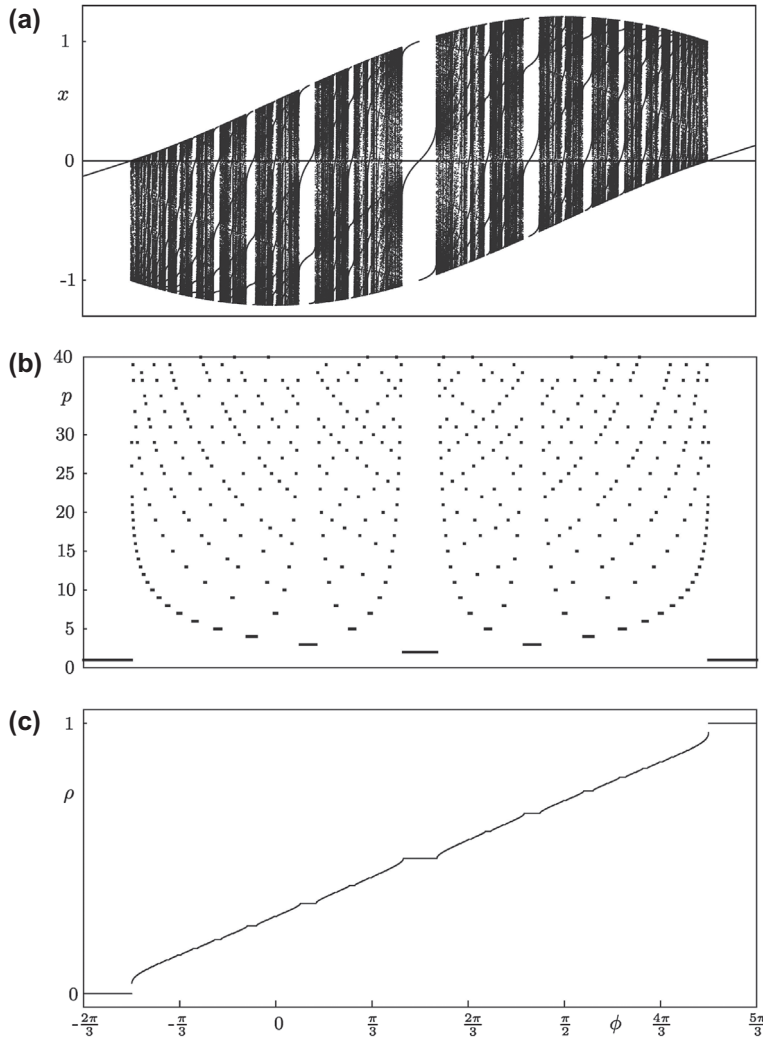


Figure 28. In (a): Bifurcation diagram of map (32) along the curve marked with C_1 in Figure 26. In (b) and (c) the period p and the rotation number ρ diagrams are shown, respectively.

As we already mentioned, the map (2), when it is a circle homeomorphism, is conjugate to a rotation map, thus, for such a map case (2) in Proposition 16 holds, where for a rational rotation any point of I is periodic, while for an irrational rotation interval I is an attractor filled with quasiperiodic orbits.

Both cases mentioned in Proposition 16 can be observed in the well-known Arnol'd circle map defined by

$$x_{n+1} = x_n + \Omega - \frac{K}{2\pi} \sin(2\pi x_n) \bmod 1 \quad (35)$$

which belongs to the family of piecewise increasing maps for $0 \leq K \leq 1$. Referring to the Arnol'd tongues (periodicity regions) in the (Ω, K) -parameter plane, recall that for a fixed $0 < K \leq 1$ there are Ω -parameter intervals corresponding to rational rotation (attracting

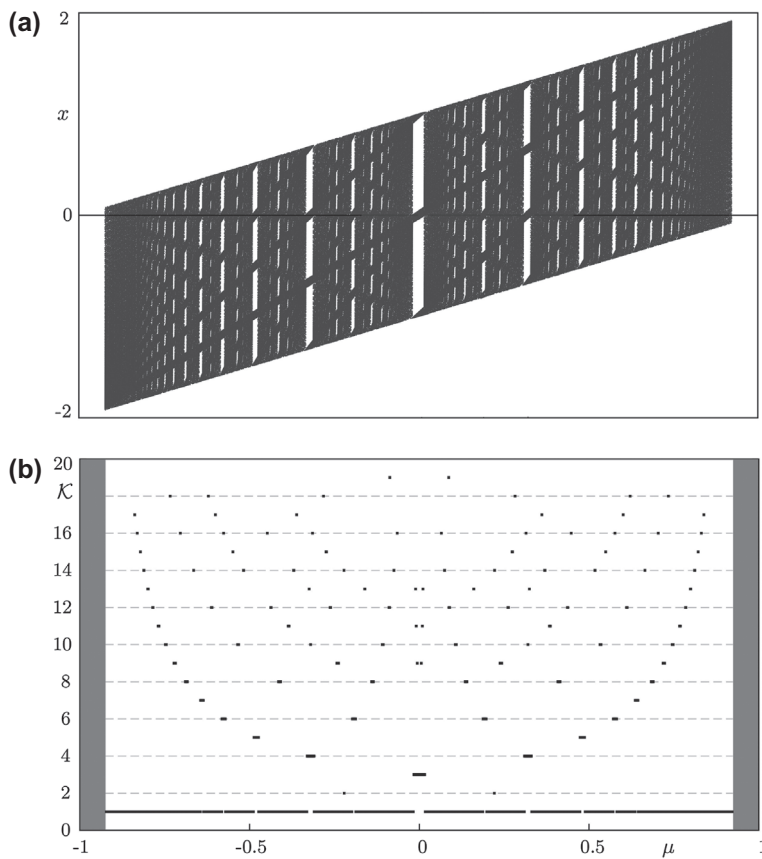


Figure 29. In (a): Bandcount adding scenario in map (2). In (b): \mathcal{K} is the number of bands. The parameter intervals indicated by grey correspond to the divergence of typical orbits. Parameters: $a_L = a_R = 1.04$, $\mu_L = \mu + 1$, $\mu_R = \mu - 1$.

cycles), and a Cantor set of values of Ω associated with irrational rotation (quasiperiodic orbits). For $K = 0$ the map is identical to the linear rotation map (34). Recall also that the Cantor set in the parameter space corresponding to irrational rotation numbers has Lebesgue measure zero at $K = 1$, and a positive measure for $0 < K < 1$ (a so-called fat Cantor set). More precisely, the measure of this Cantor set considered as a function of K is decreasing from one at $K = 0$ to zero as K approaches $K = 1$ (see, e.g. [21,25]).

Map (32) is a circle homeomorphism for parameters satisfying the condition related to (26):

$$\{(\mu_L, \mu_R) \mid \mu_L^2 + \mu_R = -\mu_R^2 + \mu_L\} \quad (36)$$

The bifurcation structure observed for parameters varied along the corresponding curve in the parameter space (denoted C_1 in Figure 26) is shown in Figure 28. As one can see, the bifurcation scenario is similar to the one we observed in the case in which map (32) is a gap map. Similar to the gap map, the rational rotation numbers cover intervals in the parameter space, while the parameter values corresponding to irrational rotation numbers form a Cantor set. The difference between these two cases regards the behaviour of the map for irrational rotation numbers. In both cases the map has an uncountable number

of quasiperiodic orbits dense on the attracting set. However, if map (32) represents a gap map, these quasiperiodic orbits belong to a Cantor set attractor, whereas if map (32) is a circle homeomorphism, they are dense in the complete absorbing interval I .

10.4. Overlapping maps

In the case of overlapping maps less general results can be proved. In the majority of cases there exists a set on which the map is chaotic (note that this set may represent a chaotic attractor or a chaotic repeller). In [49] the following Proposition is proved:

Proposition 17: *If map (24) is an overlapping map and the overlapping region Z_2 allows at least two cycles of different periods then $\rho(x)$ covers an interval $[\alpha, \beta]$ with $\alpha \neq \beta$ and, thus, there exists a set $\Lambda \subset I$ on which the map is chaotic.*

The following results are also useful to detect chaos:

Proposition 18: *If map (24) is an overlapping map and*

- (1) *it has a fixed point at one of the boundaries of interval I then there exists a set $\Lambda \subset I$ on which the map is chaotic (see [49]);*
- (2) *if the map is expanding with $f'(x) > \sqrt{2}$ for all $x \in I$, then f is chaotic in I (see [40,42]);*
- (3) *if for all $x \in I \setminus \{0\}$ it holds that $f'(x) \geq \beta > 1$ then there exists a set $\Lambda \subset I$ on which the map is chaotic (see [71]).*

There are many possibilities regarding the attractors of an overlapping map. As an example we shown in Figure 29 so-called *bandcound adding scenario* observed in map (2), which is formed by chaotic attractors only. All the bifurcations associated with this scenario are expansion bifurcations. An overlapping map may have several attracting cycles. It can also be shown that the map may have a wandering interval and therefore a Cantor set attractor [17]. Other invariant sets of overlapping maps include repelling cycles and chaotic repellers. Moreover, intervals filled with neutral cycles may appear as well.

To illustrate some possible dynamics which may occur in overlapping maps let us consider again map (32). In the case shown in Figure 30(a) it has a 3-band chaotic attractor. Additionally, at this parameter value the map has a repelling 2-cycle. In the case shown in Figure 30(b) the map has a chaotic repeller, while the attractors are given by two attracting cycles of periods 2 and 11. In fact, it can be shown that for any two periods p_1 and p_2 there exist parameter values for which map (32) has attracting p_1 - and p_2 -cycles. However, a set on which the map is chaotic does not necessarily exist. This is illustrated in Figure 30(c). At these parameter values the interval I contains two attracting 4-cycles, a repelling 4-cycle, a repelling 2-cycle and no other invariant sets. One more example is shown in Figure 30(d): at these parameter values the map has a Cantor set attractor and a repelling 2-cycle, but no chaotic set.

It is worth noting that for an overlapping map a return map may be constructed on some suitable interval (or, in other words, the map may be renormalized), which represents a gap map. In particular, this fact is used in [17] to show that an overlapping map may have a Cantor set attractor (this necessarily happens if the first return map is a gap map with an irrational rotation number).

Some examples for which the first return map for an overlapping map represents a gap map are given in Figure 30(c) and (d). In these cases the first return map defined on the

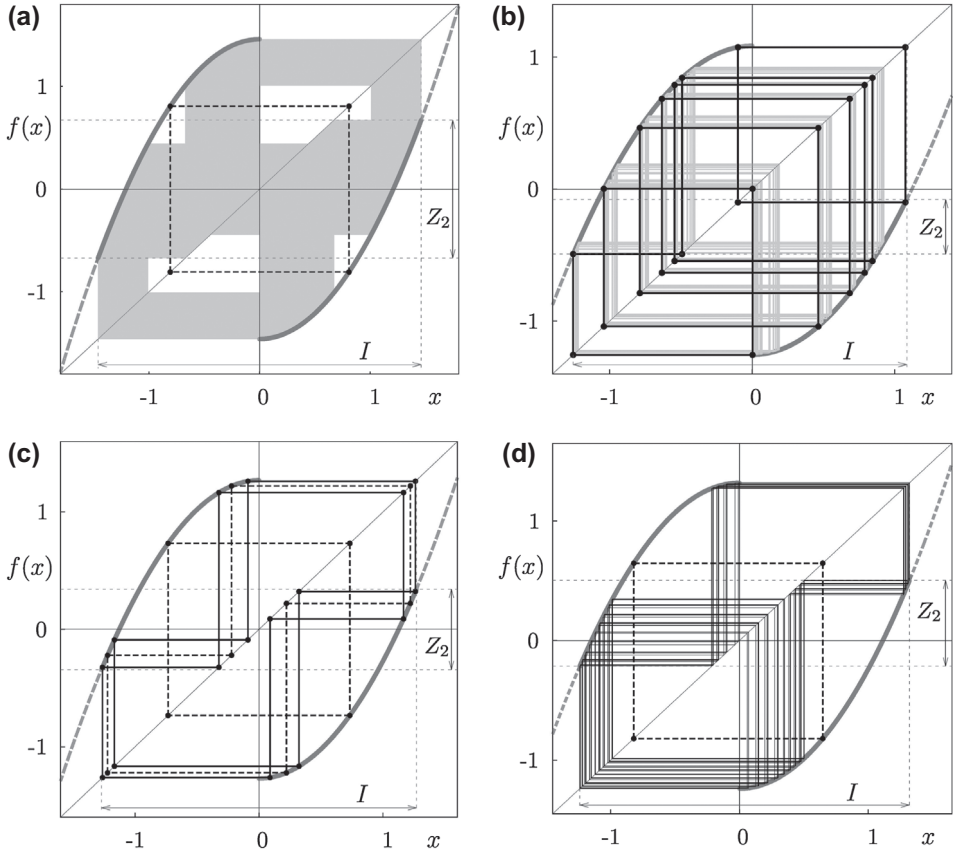


Figure 30. Invariant sets of the overlapping map (32): a chaotic 3-band attractor and a repelling 2-cycle (a); an attracting 2-cycle, an attracting 11-cycle and a chaotic repeller (b); two attracting 4-cycles, a repelling 4-cycle and a repelling 2-cycle (c); a Cantor set attractor with rotation number $\rho = \frac{\sqrt{3}}{5}$ and a repelling 2-cycle (d). Parameter values (the corresponding points are marked in Figure 26): (a) $\mu_L = 1.46$, $\mu_R = -1.46$; (b) $\mu_L = 1.08501408140814$, $\mu_R = -1.255611573157316$; (c) $\mu_L = 1.27$, $\mu_R = -1.27$; (d) $\mu_L = 1.32$, $\mu_R = -1.239017285776687$.

interval

$$J = [f_L(f_R(0)), f_R(f_L(0))] \equiv Z_2 \quad (37)$$

coincides with the second iterate of map (32) and is given by

$$x_{n+1} = g(x_n) = \begin{cases} f_R(f_L(x_n)) & \text{if } f_L \circ f_R(0) < x_n < 0 \\ f_L(f_R(x_n)) & \text{if } 0 < x_n < f_R \circ f_L(0) \end{cases} \quad (38)$$

As one can see in Figure 31, this first return map is a gap map; the gap is given by

$$Z_0 = [f_L(f_R(f_R(f_L(0)))), f_R(f_L(f_L(f_R(0))))] \quad (39)$$

The three 4-cycles of the original map correspond to the three 2-cycles of the first return map (with the rotation number $\rho = \frac{1}{2}$). Moreover, as the first return map is a gap map, all

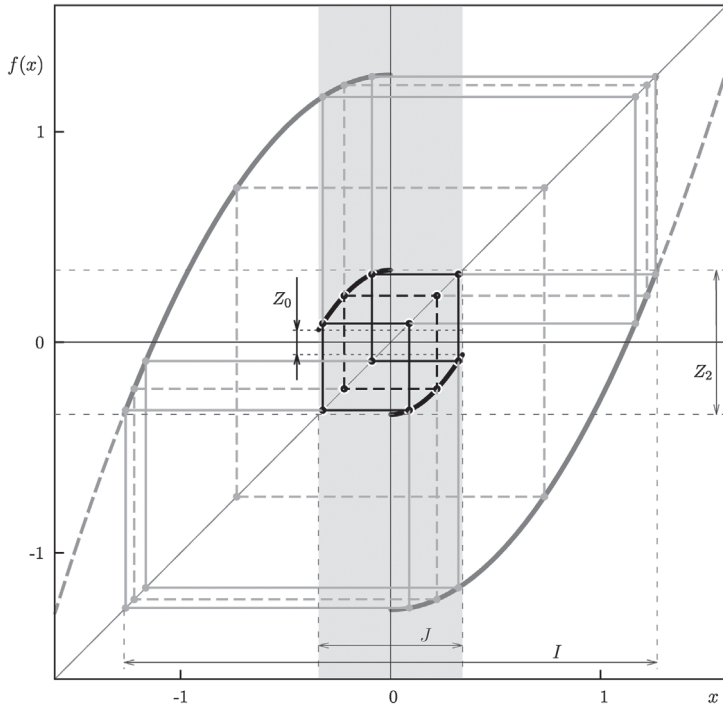


Figure 31. First return map (shown in black) for map (32) (shown in grey) defined on the interval $J = Z_2$ (marked in light grey). This first return map is a gap map; its gap is marked with Z_0 . The 4-cycles of map (32) (shown in grey) correspond to the 2-cycles of the first return map (shown in black). Attracting and repelling cycles are shown with solid and dashed lines, respectively. The parameter values are the same as in Figure 30(c).

its cycles must have the same period. This proves that the original map inside the interval Z_2 cannot have any periodic point with period different from four.

A similar situation can be observed for the case shown in Figure 30(d). Here the first return map defined on the interval Z_2 is also a gap map, but by contrast to the previous case it has an irrational rotation number.

11. Conclusions

In the present paper we discuss some basic notions and concepts, and recall several important results, associated with the dynamics of 1D discontinuous piecewise smooth maps. In fact, it is not surprising that many definitions and statements, known from the theory of smooth maps, are applicable for piecewise smooth maps without significant changes. In our survey we recall the notions which have similar definitions for 1D smooth and piecewise smooth maps, such as, for example, the definitions of an attractor and its basin of attraction, homoclinic orbit, chaotic set, first return map, and others. In the meantime, some definitions are properly modified to fit the nonsmooth case, such as, for example, the definition of a critical point or critical homoclinic orbit, and some new concepts valid only for nonsmooth maps are introduced (e.g. a BCB or a Cantor set attractor). It is clear that for a generic piecewise smooth map, especially for a discontinuous one, more rich bifurcation structures can be observed due to an interplay between smooth



and nonsmooth bifurcations, as well as due to possible robustness of chaotic attractors. As an example, we discuss the dynamics of the particular family of piecewise increasing maps, known as Lorenz maps. To give a complete classification of the various bifurcation structures observed in the parameter space of a generic 1D discontinuous map is a challenging task, and we think that the present survey will be useful for the researchers working in this field.

Notes

1. That means, a critical point associated with local extrema of a smooth function.
2. As we recall in Section 5.3, an invariant set known as *critical attractor* or *Feigenbaum attractor* (see e.g. [72]) is a Milnor attractor and not an attractor in Definition 4.
3. That means, the components of $\mathcal{B}(\mathcal{A})$ can be put in one-to-one correspondence with a Cantor set.
4. An exception is given by piecewise smooth maps with flat branches, for which the inverse is ‘interval-valued’. As a consequence, the stable set of a repelling fixed point of such maps may represent a set containing both points and intervals (see, e.g. [7]).
5. This parameter value is defined by the condition $q^3(\frac{1}{2}) = \mathcal{O}_R$ and is given by $\bar{\alpha}_1 = \frac{2}{3} \left(\sqrt{19 + 3\sqrt[3]{33}} + \frac{4}{\sqrt{19 + 3\sqrt[3]{33}}} + 1 \right) \approx 3.678573511$.
6. Clearly a noncritical homoclinic orbit may be degenerate or nondegenerate, while a nondegenerate homoclinic orbit is also noncritical.
7. Note that the definition of robustness given in [13] includes the uniqueness of the chaotic attractor, since this feature may be quite important for engineering reasons. This property is not required by our definition. On the other hand, the persistence of the geometrical structure of a chaotic attractor (the number of its bands) is not required by the definition given in [13].
8. Note that the Poincaré return maps of Lorenz-like flows do not necessarily lead to maps of this class. Depending on the properties of the flow, Poincaré return maps with one or two decreasing branches are possible as well (see, e.g. [52]).

Acknowledgements

The work of L. Gardini and I. Sushko has been performed under the auspices of the COST action IS1104 ‘The EU in the new economic complex geography: models, tools and policy evaluation’, www.gecomplexitycost.eu. L. Gardini acknowledge also the GNFM (National Group of Mathematical Physics, INDAM Italian Research Group). I. Sushko thanks also University of Urbino for the hospitality during her stay there as a Visiting Professor.

Disclosure statement

No potential conflict of interest was reported by the authors.

Funding

The work of V. Avrutin was partially supported by the German Research Foundation within the scope of the project ‘Organizing centers in discontinuous dynamical systems: bifurcations of higher codimension in theory and applications’.

References

- [1] P. Aghion, A. Banerjee, and T. Piketty, *Dualism and macroeconomic volatility*, Q. J. Econ. 114 (1999), pp. 1359–1397.
- [2] D. Assaf and S. Gadbois, *Definition of chaos*, Lett. Amer. Math. Monthly 99 (1992), p. 865.
- [3] V. Avrutin, B. Eckstein, and M. Schanz, *On detection of multi-band chaotic attractors*, Proc. R. Soc. A 463 (2007), pp. 1339–1358.
- [4] V. Avrutin, B. Eckstein, and M. Schanz, *The bandcount increment scenario. I: Basic structures*, Proc. R. Soc. A 464 (2008), pp. 1867–1883.
- [5] V. Avrutin, B. Eckstein, and M. Schanz, *The bandcount increment scenario. II: Interior structures*, Proc. R. Soc. A 464 (2008), pp. 2247–2263.
- [6] V. Avrutin, B. Eckstein, and M. Schanz, *The bandcount increment scenario. III: Deformed structures*, Proc. R. Soc. A 465 (2009), pp. 41–57.
- [7] V. Avrutin, B. Futter, and M. Schanz, *The discontinuous flat top tent map and the nested period incrementing bifurcation structure*, Chaos Solitons Fractals 45 (2012), pp. 465–482.
- [8] V. Avrutin, L. Gardini, M. Schanz, and I. Sushko, *Bifurcations of chaotic attractors in one-dimensional maps*, Int. J. Bifur. Chaos 24 (2014), pp. 1440012-1–1440012-10.
- [9] V. Avrutin and M. Schanz, *On the fully developed bandcount adding scenario*, Nonlinearity 21 (2008), pp. 1077–1103.
- [10] V. Avrutin, M. Schanz, and L. Gardini, *Self-similarity of the bandcount adding structures: Calculation by map replacement*, Regul. Chaotic Dyn. 15 (2010), pp. 685–703.
- [11] V. Avrutin, I. Sushko, and L. Gardini, *Cyclicity of chaotic attractors in one-dimensional discontinuous maps*, Math. Comput. Simul. (Special Issue “Discontinuous Dynamical Systems: Theory and Numerical Methods”) 95 (2014), pp. 126–136.
- [12] S. Banerjee and G.C. Verghese, *Nonlinear Phenomena in Power Electronics – Attractors, Bifurcations, Chaos, and Nonlinear Control*, Wiley-IEEE Press, 2001.
- [13] S. Banerjee, J.A. Yorke, and C. Grebogi, *Robust chaos*, Phys. Rev. Lett. 80 (1998), pp. 3049–3052.
- [14] J. Banks, J. Brooks, G. Cairns, G. Davis, and P. Stacey, *On Devaney’s definition of chaos*, Amer. Math. Monthly 99 (1992), pp. 332–334.
- [15] M. di Bernardo, C.J. Budd, A.R. Champneys, and P. Kowalczyk, *Piecewise-smooth Dynamical Systems: Theory and Applications*, Applied Mathematical Sciences Vol. 163, Springer, London, 2008.
- [16] M. di Bernardo, M.I. Feigin, S.J. Hogan, and M.E. Homer, *Local analysis of C-bifurcations in n-dimensional piecewise smooth dynamical systems*, Chaos Solitons Fractals 10 (1999), pp. 1881–1908.
- [17] D. Berry and B. Mestel, *Wandering interval for Lorenz maps with bounded nonlinearity*, Bull. Lond. Math. Soc. 23 (1991), pp. 183–189.
- [18] G.I. Bischi, C. Chiarella, M. Kopel, and F. Szidarovszky, *Nonlinear Oligopolies: Stability and Bifurcations*, Springer, Heidelberg, 2009.
- [19] G.I. Bischi, C. Mira, and L. Gardini, *Unbounded sets of attraction*, Int. J. Bifur. Chaos 10 (2000), pp. 1437–1469.
- [20] L.S. Block and W.A. Coppel, *Dynamics in One Dimension*, Springer Lecture Notes Vol. 1513, Springer Verlag, Berlin Heidelberg, 1992.
- [21] P. Boyland, *Bifurcations of circle maps: Arnol’d tongues, bistability and rotation intervals*, Commun. Math. Phys. 106 (1986), pp. 353–381.
- [22] B. Brogliato, *Nonsmooth Mechanics – Models, Dynamics and Control*, Springer-Verlag, New York, 1999.
- [23] J. Buescu and I. Stewart, *Liapunov stability and adding machines*, Ergodic Theory Dyn. Syst. 15(02) (1995), pp. 271–290.
- [24] P.C. Coullet, J.M. Gambaudo, and C. Tresser, *Une nouvelle bifurcation de codimension 2: le collage de cycles* [A new bifurcation of codimension 2: The gluing of cycles], C. R. Acad. Sci. Paris, Série I 299 (1984), pp. 253–256.
- [25] P. Cvitanović, *Universality in Chaos*, Adam Hilger Ltd., Bristol, 1984.

- [26] A. Denjoy, *Sur les courbes definies par les équations différentielles a la surface du tore* [On the curves defined by the differential equations on the surface of the torus], J. Math. Pure Appl. 11 (1932), pp. 333–375.
- [27] R.L. Devaney, *An Introduction to Chaotic Dynamical Systems*, The Benjamin/Cummings Publishing Corporation, Menlo Park, CA, 1986.
- [28] R.L. Devaney, *An Introduction to Chaotic Dynamical Systems*, 2nd ed., Addison-Wesley, Redwood City, 1989.
- [29] P. Fatou, *Mémoire sur les équations fonctionnelles* [A note on functional equations], Bull. Soc. Math. France 47 (1919), pp. 161–271.
- [30] M.I. Feigin, *Doubling of the oscillation period with C-bifurcations in piecewise-continuous systems*, Prikl. Math. Mekh. 34 (1970), pp. 861–869 (in Russian).
- [31] J.M. Gambaudo, P. Glendinning, and C. Tresser, *Collage de cycles et suites de Farey* [Gluing of cycles and Farey series], C. R. Acad. Sci. Paris, Série I 299 (1984), pp. 711–714.
- [32] J.M. Gambaudo, I. Procaccia, S. Thomae, and C. Tresser, *New universal scenarios for the onset of chaos in Lorenz-type flows*, Phys. Rev. Lett. 57 (1986), pp. 925–928.
- [33] L. Gardini, V. Avrutin, and I. Sushko, *Codimension-2 border collision bifurcations in one-dimensional discontinuous piecewise smooth maps*, Int. J. Bifurcat. Chaos 24 (2014), pp. 1450024-1–1450024-30.
- [34] L. Gardini, I. Sushko, V. Avrutin, and M. Schanz, *Critical homoclinic orbits lead to snap-back repellers*, Chaos Solitons Fractals 44 (2011), pp. 433–449.
- [35] L. Gardini, I. Sushko, and A. Naimzada, *Growing through chaotic intervals*, J. Econ. Theory 143 (2008), pp. 541–557.
- [36] L. Gardini, F. Tramontana, V. Avrutin, and M. Schanz, *Border collision bifurcations in 1D piecewise-linear maps and Leonov's approach*, Int. J. Bifurcat. Chaos 20 (2010), pp. 3085–3104.
- [37] R. Ghrist, *Resonant gluing bifurcations*, Int. J. Bifur. Chaos 10 (2000), pp. 2141–2160.
- [38] R. Ghrist and P.J. Holmes, *Knots and orbit genealogies in three dimensional flows*, in *Bifurcations and Periodic Orbits of Vector Fields*, Kluwer Academic, 1993, pp. 185–239.
- [39] R. Ghrist and P.J. Holmes, *Knotting within the gluing bifurcation*, in *IUTAM Symposium on Nonlinearity and Chaos in the Engineering Dynamics*, J.M.T. Thompson and S.R. Bishop, eds., John Wiley Press, 1994, pp. 299–315.
- [40] P. Glendinning, *Topological conjugation of Lorenz maps to β -transformations*, Math. Proc. Camb. Phil. Soc. 107 (1990), pp. 401–413.
- [41] J. Guckenheimer and P.J. Holmes, *Nonlinear Oscillations, Dynamical Systems and Bifurcations of Vector Fields*, 4th ed., Applied Mathematical Sciences, Springer, New York, 1983.
- [42] F. Hofbauer, *The maximal measure for linear mod one transformations*, J. Lond. Math. Soc. (2) 23 (1981), pp. 92–112.
- [43] A.J. Homburg, *Global aspects of homoclinic bifurcations of vector fields*, Springer-Verlag, Berlin, 1996.
- [44] J.H. Hubbard and C.T. Sparrow, *The classification of topologically expansive Lorenz maps*, Commun. Pure Appl. Math. XLIII (1990), pp. 431–443.
- [45] S. Ito, S. Tanaka, and H. Nakada, *On unimodal transformations and chaos II*, Tokyo J. Math. 2 (1979), pp. 241–259.
- [46] M. Jakobson, *Absolutely continuous invariant measures for one-parameter families of one-dimensional maps*, Commun. Math. Phys. 81 (1981), pp. 39–88.
- [47] K.L. Judd, *On the performance of patents*, Econometrica 53 (1985), pp. 567–586.
- [48] G. Julia, *Mémoire sur l'itération des fonctions rationnelles* [A note on the iteration of rational functions], J. Math. Pures Appl., 7ème série 4 (1918), pp. 47–245.
- [49] J.P. Keener, *Chaotic behavior in piecewise continuous difference equations*, Trans. Amer. Math. Soc. 261 (1980), pp. 589–604.
- [50] N.N. Leonov, *On a pointwise mapping of a line into itself*, Radiofisika 2 (1959), pp. 942–956 (in Russian).
- [51] T. Li and J. Yorke, *Period three implies chaos*, Amer. Math. Monthly 82 (1975), pp. 985–992.

- [52] D.V. Lyubimov, A.S. Pikovsky, and M.A. Zaks, *Universal scenarios of transitions to chaos via homoclinic bifurcations*, Math. Phys. Rev. 8 (1989). Harwood Academic, London. Russian version as a Preprint (192) of Russian Academy of Science, Institute of Mechanics of Solid Matter, 1986, Sverdlovsk.
- [53] Y.L. Maistrenko, V.L. Maistrenko, and L.O. Chua, *Cycles of chaotic intervals in a time-delayed Chua's circuit*, Int. J. Bifur. Chaos 3 (1993), pp. 1557–1572.
- [54] F. Marotto, *Snap-back repellers imply chaos in R^n* , J. Math. Anal. Appl. 63 (1978), pp. 199–223.
- [55] F. Marotto, *On redefining a snap-back repeller*, Chaos Solitons Fractals 25 (2005), pp. 25–28.
- [56] K. Matsuyama, *Growing through cycles*, Econometrica 67 (1999), pp. 335–347.
- [57] K. Matsuyama, *Financial market globalization, symmetry-breaking, and endogenous inequality of nations*, Econometrica 72 (2004), pp. 853–884.
- [58] K. Matsuyama, *Credit traps and credit cycles*, Amer. Econ. Rev. 97 (2007), pp. 503–516.
- [59] K. Matsuyama, *The good, the bad, and the ugly: An inquiry into the causes and nature of credit cycles*, Theor. Econ. 8 (2013), pp. 623–651.
- [60] K. Matsuyama, I. Sushko, and L. Gardini, *Globalization and synchronization of innovation cycles*, Geocomplexity: Discussion Papers Series, No. 9/2015, 2015.
- [61] K. Matsuyama, I. Sushko, and L. Gardini, *Revisiting the model of credit cycles with good and bad projects*, J. Econ. Theory 163 (2016), pp. 525–556.
- [62] I. Melbourne, M. Dellnitz, and M. Golubitsky, *The structure of symmetric attractors*, Arch. Ration. Mech. Anal. 123 (1993), pp. 75–98.
- [63] W. de Melo and S. van Strien, *One-dimensional Dynamics*, Springer, New York, 1991.
- [64] J.W. Milnor, *On the concept of attractor*, Commun. Math. Phys. 99 (1985), pp. 177–195.
- [65] C. Mira, *Chaotic Dynamics: From the One-dimensional Endomorphism to the Two-dimensional Diffeomorphism*, World Scientific, Singapore, 1987.
- [66] C. Mira, L. Gardini, A. Barugola, and J.C. Cathala, *Chaotic Dynamics in Two-dimensional Noninvertible Maps*, World Scientific Series on Nonlinear Science Vol. 20, World Scientific, Singapore, 1996.
- [67] H.E. Nusse and J.A. Yorke, *Border-collision bifurcations including 'period two to period three' bifurcation for piecewise smooth systems*, Physica D 57 (1992), pp. 39–57.
- [68] H.E. Nusse and J.A. Yorke, *Border-collision bifurcations for piecewise smooth one dimensional maps*, Int. J. Bifur. Chaos 5 (1995), pp. 189–207.
- [69] H. Poincaré, *Mémoire sur les courbes définies par une équation différentielle* [A note on the curves defined by a differential equation], J. Math. 7 (1881), pp. 375–422.
- [70] I. Procaccia, S. Thomae, and C. Tresser, *First-return maps as a unified renormalization scheme for dynamical systems*, Phys. Rev. A 35 (1987), pp. 1884–1900.
- [71] R.C. Robinson, *An Introduction to Dynamical Systems: Continuous and Discrete*, American Mathematical Society, 2012.
- [72] A. Sharkovsky, S. Kolyada, A. Sivak, and V. Fedorenko, *Dynamics of One-dimensional Maps*, Kluwer Academic, Dordrecht, 1997.
- [73] I. Sushko, A. Agliari, and L. Gardini, *Bistability and border-collision bifurcations for a family of unimodal piecewise smooth maps*, Discrete Contin. Dyn. Syst. Ser. B 5 (2005), pp. 881–897.
- [74] I. Sushko, A. Agliari, and L. Gardini, *Bifurcation structure of parameter plane for a family of unimodal piecewise smooth maps: Border-collision bifurcation curves*, Chaos Solitons Fractals 29 (2006), pp. 756–770.
- [75] I. Sushko, V. Avrutin, and L. Gardini, *Bifurcation structure in the skew tent map and its application as a border collision normal form*, J. Differ. Equ. Appl. (2015). doi: 10.1080/10236198.2015.1113273
- [76] I. Sushko and L. Gardini, *Degenerate bifurcations and border collisions in piecewise smooth 1D and 2D maps*, Int. J. Bifur. Chaos 20 (2010), pp. 2045–2070.
- [77] D.V. Turaev and L.P. Shil'nikov, *On bifurcations of a homoclinic "Figure of Eight" for a saddle with a negative saddle value*, Soviet Math. Dokl. 34 (1987), pp. 397–401 (Russian version 1986).
- [78] M. Vellekoop and R. Berglund, *On intervals, transitivity = chaos*, Amer. Math. Monthly 101 (1994), pp. 353–355.

- [79] D. Yiming and F. Wentao, *The asymptotic periodicity of Lorenz maps*, Acta Math. Sci. 19 (1999), pp. 114–120.
- [80] Zh.T. Zhusubaliyev and E. Mosekilde, *Bifurcations and Chaos in Piecewise-smooth Dynamical Systems*, Nonlinear Science A Vol. 44, World Scientific, 2003.